CHAPTER 12

Transfer-printed devices for biomedical applications

Changbo Liu[1,2] **and Xing Sheng**[3]
[1]School of Materials Science and Engineering, Beihang University, Beijing, P.R. China
[2]Hangzhou Innovation Institute, Beihang University, Hangzhou, P.R. China
[3]Department of Electronic Engineering, Tsinghua University, Beijing, P.R. China

12.1 Introduction

As an emerging manufacturing technique, the "transfer printing" method provides opportunities for the integration of brittle inorganic electronic materials and organic flexible/stretchable substrates. Transfer printing processes provide versatile routes to high-performance, heterogeneously integrated functional systems, including those in flexible electronics, three-dimensional (3D) and/or curvilinear optoelectronics, and biointegrated sensing and therapeutic devices (Carlson et al., 2012). This method can integrate brittle inorganic electronic materials and devices onto nearly any type of substrate including but not limited to rubber, plastic, and fabric (Khang et al., 2006). The most appealing feature of this approach is that the majority of the manufacturing process involves conventional fabrication technology, which already has a mature, established commercial infrastructure, thereby accelerating time toward commercialization and practical applications (Rogers et al., 2016).

Recent advances in material sciences and microfabrication technologies have enabled the creation of flexible and stretchable inorganic electronics, which are fabricated based on microfabrication including film deposition, lithography, and most importantly transfer printing technology (Chen et al., 2020). The performance of flexible electronic devices is almost the same as that of their conventional counterparts, which is attributed to the fact that transfer printing is relatively benign, and it conserves the performance metrics of the source materials. This not only preserves the high-performance characteristics but also makes the devices flexible or stretchable depending on the material of the target substrate. Compared with traditional Si-based electronics, flexible inorganic electronics offer several advantages: they are soft, deformable, foldable, lightweight, portable, and can be manufactured using less expensive methods (Mostafalu et al., 2016). These unique characteristics make them excellent for applications that require smaller footprints or possess surfaces with curvilinear and irregular morphology. Flexible electronics can be bent, twisted, and wrapped

Transfer Printing Technologies and Applications
DOI: https://doi.org/10.1016/B978-0-443-18845-9.00012-0

around irregularly shaped objects without losing their functionalities, which provides an array of opportunities for application in the biomedical field, such as controlling disease conditions, improving surgical procedures, continuous health monitoring, and so on. The electronic devices, which are transferred onto the flexible substrate, can conformal to the curved biotissue surface and dynamically adapt to the tissue's deformation, the signal-to-noise ratio (SNR) and spatial resolution have been much improved compared with the conventional counterparts. One of the promising applications of flexible electronics that could not be addressed with conventional technology includes advanced wireless biomedical devices, especially implantable and wearable medical electronics. We can collect, and analysis of biological signals related to the physiological health status by wrapping (or implanting into) the brain with them or putting them on the skin to achieve an intimate interface with the body.

In the past decade, flexible inorganic electronics have received and continuously attracted attention from academia and industry due to their wide potential applications in the biomedical area. Many emerging bioelectronics systems have become increasingly popular due to exciting characteristics, such as wearable electronics, flexible implantable electronics, electronic tattoos, and electronic skin. With the rapid development of flexible electronics, the transfer printing technique has also been greatly improved, including the range of materials for patterning the and scope of applications enabled. At present, transfer printing has developed into a sophisticated approach to materials assembly and device fabrication creates opportunities for a wide range of device platforms over conventional manufacturing or growth techniques. Transfer printing has broad substrate applicability and materials versatility. Essentially any class of material or device can be integrated onto the foreign substrate using transfer printing-based fabrication schemes: from two-dimensional (2D) materials (carbon nanotubes, graphene, Maxene, etc.) high-performance hard materials (metals, oxide thin films, single-crystalline/noncrystalline inorganic semiconductors, etc.), to biomaterials (DNA, protein, viruses, cell, etc.), to fully integrated device structures [thin film transistors (TFTs), light emitting diodes (LEDs), photodetector (PD), complementary metal oxide semiconductor (CMOS) circuits, sensing arrays, solar cells, energy-harvesting devices, etc.]. Additionally, transfer printing enables the cointegration of dissimilar materials: single-crystalline materials with various lattice constants and noncrystalline materials; those with high and low thermal stability; those with high and low moduli, and so on (Yoon et al., 2015).

In this chapter, we introduce the recent advance in heterogeneously integrated materials and integrated inorganic devices for biomedical applications. The first part of the chapter describes materials including metals, oxides, silicon, wide bandgap semiconductors, 2D materials, and biomaterials. The second part of the chapter describes functional devices including LEDs, PD, energy-harvesting devices, and bioresorbable materials and devices. This chapter introduces different fabrication methods for flexible bioelectronics and discusses their working mechanism.

12.2 Materials

12.2.1 Metals

Metal materials have been in use as biomaterials for a long time due to their excellent yield strength and biocompatibility. In recent years, with the development of transfer printing technology, metal materials are also widely integrated with flexible substrates to form flexible bioelectronic devices, which have unique performance over traditional brittle metal devices. Metal materials are considered superior candidates for preparing electrodes, electrical interconnection wires, antennas, and stress-sensor due to excellent conductivity, electrical stability, and mature preparation technology. Metal films can be transferred onto flexible substrates to get bendable, stretchable, twistable electrodes or antenna structures for electrical stimulation, electrophysiological signal collection, or wireless transmission.

Flexible electrodes provide a perfect contact interface for electrophysiological monitoring. The Au film is chosen as the electrode material in most flexible electronics for its biocompatibility, chemical inertness, as well as ductility. As shown in Fig. 12.1A, *left* photo, a stretchable neural electrocorticography (ECoG) electrode array, which consists of nine channels with a three-layered serpentine-like interconnect structure, is fabricated by transferring Au conductive layer onto the polydimethylsiloxane (PDMS) substrate (Yan et al., 2017). The transferred Au conductive layer includes three parts: the output part, the serpentine interconnector, and signal collection. Nine small circles, serving as signal collect parts, are connected to the output part (nine parallel square pads to connect to the ECoG recorder) via the serpentine interconnectors. To improve the mechanical stability of the ECoG electrode array during deformation, the Au conductive layer is located at the neutral mechanical plane of the two PI films. The ability of the stretchable electrode array to conform to different curved surfaces is confirmed by the experiment. The right figure shows an optical image of a stretchable neural electrode array placed on the visual cortical surface of the left hemisphere of a rat. The surgeries in a rat have demonstrated that the stretchable electrode array maintained perfect contact against the curved surface of the brain in the rat, and high-quality ECoG signals from anesthetized rats are collected. The application of the stretchable electrode array on the detection of steady-state visual evoked potentials (SSVEPs) response has also been demonstrated by in vivo experiments, the results indicated that SSVEP responses recorded by the stretchable neural electrode array are more obvious than those detected by traditional stainless-steel screw electrodes (Yan et al., 2017). In addition, Au film can also be integrated with the ultra-thin flexible substrate to get epidermal electronic systems (EESs), which are ultra-thin and ultra-soft electronics, sensors, and actuators, whose physical properties (modulus, thickness, and areal mass density) match well with those of human epidermis (Kim et al., 2011; Wang et al., 2018; Yeo et al., 2013). Fig. 12.1B shows a representative EES based on

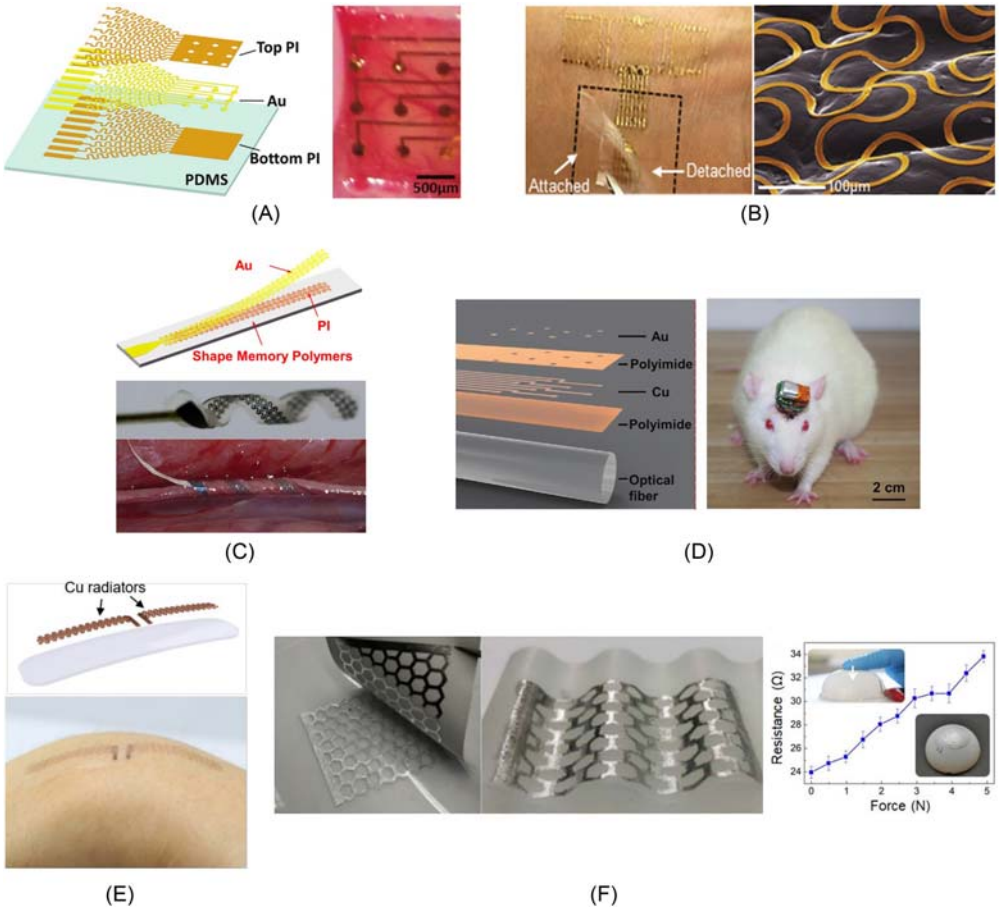

Figure 12.1 Metal materials: (A) Transfer Au film onto elastomer substrate for in vivo ECoG measurement (*Left*: exploded view schematic diagram of the electrode array layout; *Right*: Optical image of a neural electrode array placed on the visual cortical surface of the left hemisphere of a rat). (B) The electronic tattoo sensors based on transferred Au film (*Left*: image of an epidermal electronic systems (EES) on skin; *Right*: colorized SEM image of an EESs mounted on the skin replica). (C) A 3D twining electrode by integrating stretchable mesh serpentine Au wires onto a flexible shape memory substrate (*Upper* and *middle*: the exploded view and optical image of the twining electrode; *Bottom*: the image of an implanted twining electrode). (D) Transfer Cu/Au microelectrode array onto the optical fibers for implantable neurological stimulation and monitoring (*Left*: the exploded view of the device; *Right*: a rat implanted with the device). (E) The wearable compliant antennas based on transferred Cu films (*Upper*: illustration showing multilayered structures for the antenna; *Bottom*: direct integration of an antenna on the wrist). (F) The transfer printing method of liquid metal for 3D wiring in flexible electronics (*Left* and *middle*: liquid-metal on planar and wavy soft substrates; *Right*: the liquid-metal stress-sensor and Resistance-Force curve). *(A) Reproduced with permission; Copyright © 2017 The Authors. Published by WILEY-VCH Verlag GmbH & Co. KGaA, Weinheim; (B) Reproduced with permission; Copyright © 2013 WILEY-VCH Verlag GmbH & Co. KGaA, Weinheim; (C) Reproduced with permission; Copyright © 2019 The Authors, some rights reserved; exclusive licensee American Association for the Advancement of Science; (D) Reproduced with permission; Copyright © 2020 Wiley-VCH GmbH; (E) Reproduced with permission; Copyright © 2020, American Chemical Society); (F) Reproduced with permission; Copyright © 2020, American Chemical Society.*

transferred Au film for monitoring electrophysiological signals (Yeo et al., 2013). The EES consists of an interconnected collection of thin, filamentary serpentine conductive traces and electrophysiological sensors, all in an open mesh layout with exposed metal (Au) that contacts the skin directly. The total thickness of the EES is only approximately 0.8 μm, in its thickest region. The top and bottom layers of PI (each 0.3 μm thick) placed the Au-based active sensing components in the neutral mechanical plane. Such designs provide the EES with extremely low effective elastic moduli and large deformability. These characters allow the EES to follow the contoured surfaces and time-dynamic motions of the skin in a natural way, which can minimize interfacial slippage and as a result, motion artifacts. Putting the EES on the skin can get conformal contact and adequate adhesion based on van der Waals interactions alone, in a manner that is without mechanical constraints for the user. As shown in Fig. 12.1B, *right*, the EES layout follows the topography of the skin including the deepest creases and pits. This conformal coverage on the skin not only seriously improves the mechanical robustness of integration, but also enlarges the contact area between the EES and the skin, which can minimize contact impedances and enables precision measurements for the case of electrophysiological.

Au film can also be integrated with new smart materials by transfer printing method and get exciting performance. Zhang et al. develop a 3D twining electrode for peripheral nerve stimulation and recording, which are fabricated by integrating stretchable mesh serpentine wires (Au) onto a flexible shape memory substrate (Zhang, Zheng, et al., 2019). The key substrate materials are shape memory polymers (SMPs), which have the dual-shape capability and can change their shape in a predefined way from shape A to shape B when exposed to an appropriate stimulus (Behl & Lendlein, 2007). Based on this feature, a 3D electronic system can be fabricated by traditional 2D planar processing and transfer printing technology. The layout of the 3D twining electrode is shown in Fig. 12.1C. The thermo-responsive SMP with a transition temperature of approximately 37°C is chosen to be the substrate. Au film with mesh serpentine structure is transferred onto the SMP substrate. After the transfer printing process, heating up and deforming the initial 2D planar assembly leads to the reconfiguration of the permanent shape to the desired 3D helical shape to match the 3D peripheral nerves. Before surgical implantation, the twining electrodes are temporarily flattened to a 2D planar state. Driven by 37°C, the temporarily flattened electrode can automatically climb onto the nerve to restore its permanent spiral structure and form 3D flexible neural interfaces. Conformal contact can lead to lower interfacial impedance, and stimulation efficiency and the recorded SNR will be improved. Additionally, no additional surgical fixation is required in the whole installation process, which can greatly reduce the nerve injury associated with the mechanical and geometrical mismatches and the surgical implantation. This twining electrode has great potential in both clinical practice and basic neuroscience research.

Transfer printing technology can integrate functional materials and devices onto nearly any type of substrate with different material properties and different surfaces. Compared with traditional electronics manufacturing techniques, the Transfer printing method makes it easy for electronics to be integrated onto complex 3D surfaces, which will greatly expand the functions and applications of electronic devices. As shown in Fig. 12.1D (Yu et al., 2021). A multichannel flexible optoelectronic fiber, which consists of flexible fibers and Cu/Au microelectrode array, is reported for implantable neurological stimulation and monitoring. The Cu/Au microelectrode array located at the neutral mechanical plane of the two PI films is transferred and printed onto the curved surface of the optical fibers by elastomer stamps and gets conformal contact with the optical fiber. The flexible optoelectronic fiber device offers multiple stimulations and sensing channels, allowing optical stimulation in selective wavelengths guided by the optical fibers while conducting distributed, high-throughput biopotential sensing using the flexible microelectrode arrays. Animal experiments have confirmed the capability of the optoelectronic fiber to conduct closed-loop neuromodulation. Using the same transfer printing method, various flexible electronic devices with complex functions can be integrated with optical fibers, and optoelectronic fibers with more advanced and sophisticated functions can be fabricated in the future.

In the biomedical field, metal materials are not only used as electrodes but also ideal materials for fabricating antennas due to their excellent conductivity. Antennas play an important role in wireless communication and remote sensing. There are huge demands for various types of antennas for bioelectronics, the internet of things, and smart healthcare. Flexible antennas have been considered a feasible solution for emerging on- and intra-body wearable bioelectronics to establish remote data transfer. Fig. 12.1E shows a stretchable dipole antenna fabricated by transfer printing technology (Kim et al., 2020). The key functional component is Cu film with 2D serpentine patterns, which is transferred onto elastomer substrates. The stretchable dipole antenna shows highly compliant mechanical characteristics and has a conformal coverage on challenging locations, such as wrists, elbows, and knees. Benefiting from excellent mechanical stretchability and low effective moduli, the dipole antenna on the wrist (bottom photo) shows no delamination with repetitive flexion. The electromagnetic properties of the stretchable antennas are characterized by both simulation and experiment to verify the stable functionalities of the antenna even in the stretched state. These stretchable antennas can be integrated with various wearable devices for long-range wireless data communication.

Liquid metal is a liquid-state metallic material with a low melting point at or around room temperature. Liquid metal is investigated as a highly desirable candidate in biosensors due to its high electrical conductivity, low toxicity, and superior fluidity. The liquid metal can achieve stable electrical signal transmission under deformation of approximately

700% (Zhang, Wang, et al., 2020). Additionally, their self-healing quality enables liquid metal with stronger durability and robustness which are essential for biosensors. As illustrated in Fig. 12.1F, A liquid–metal honeycomb circuit is fabricated on soft paper, and then transferred onto Ecoflex substrates with planar (left) and wavy surface (middle) (Zhao et al., 2020). The liquid–metal circuit on Ecoflex substrates possesses high stability and good conductivity. A piezoresistive stress sensor is fabricated by transferring a liquid metal circuit onto a flexible model with an uneven surface (spherical) to form a conformal 3D circuit (right), which benefits from the cross-section of liquid metal lines can be reduced when pressed leading to a rise in resistance. The resistance-force curve shows a good relationship between resistance and stress.

12.2.2 Oxides

The broad spectrum of physical and chemical properties in oxide materials has attracted intensive research interest in recent years. Various solid-state oxide materials have been investigated for flexible bioelectronics, such as VO_2, TiO_2, MgO, ZnO, SiO_2, and so on. Most high-performance oxide materials are prepared at high temperatures, which is incompatible with the flexible substrate. Fortunately, transfer printing technology can solve this problem, and then emerging various flexible electronics based on oxides (Fig. 12.2).

Vanadium dioxide (VO_2)-based flexible breath sensor is reported, which can conformal coverage on the skin under different curvatures and temperatures through day and night (shown in Fig. 12.2A) (Liao et al., 2017). VO_2 film is fabricated on SiO_2/Si substrate, and then transferred onto PI substrate and encapsulated with PDMS. This structure enables the sensor with robust electrical characteristics for body movements. The PDMS layer facilitated nonirritation skin bonding, and the PI layer enable isolation of the VO_2 material from applied tensile strain introduced from body movements. The breath sensor shows high sensitivity and ultrafast response time benefits from the high-temperature coefficient of resistance of VO_2 film. The results of real-time breath monitoring demonstrated that the VO_2-based flexible breath sensor is feasible for the flexible sensitive device in the apnea detection field.

Titanium dioxide (TiO_2) has remarkable properties involving chemical stability, negligible protein denaturation, and biocompatibility, and is an excellent candidate for biosensing. Lee et al. report a technology that can transfer electrospinning TiO_2 nanofibers to any target surface using a thin PDMS adhesive layer. Fig. 12.2B shows the TiO_2-based sensor for protein detection from whole blood (Lee et al., 2015). The sensor is fabricated by integrating TiO_2 nanofibers with a PC disk and affords a significant improvement in sensitivity with a broad dynamic range. The detection limits are approximately 300-fold lower than the conventional detection technique. With this transfer-printing technology, we can fully utilize the excellent properties of TiO_2 in flexible bioelectronics.

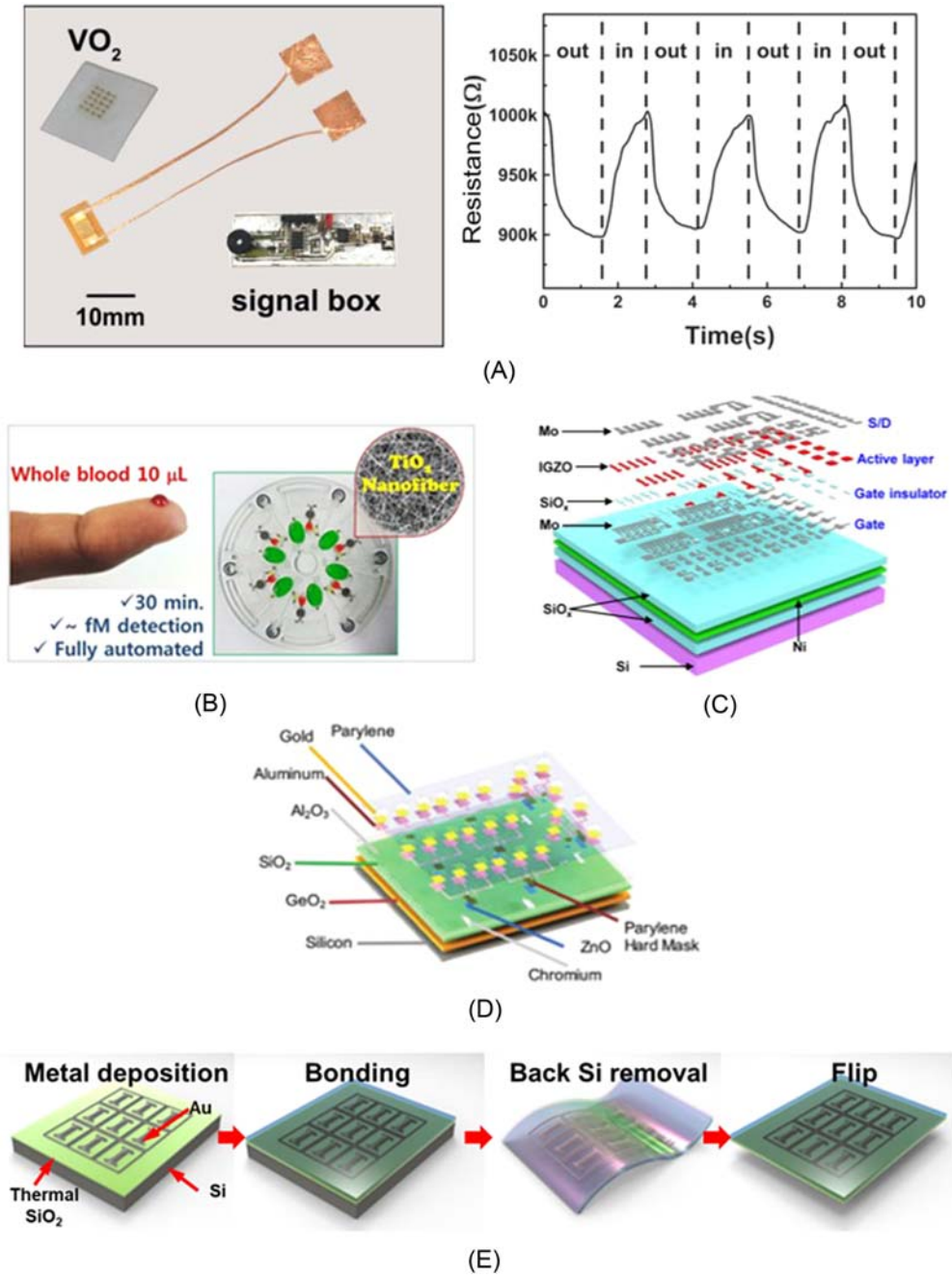

Figure 12.2 Oxides. (A) The flexible breath sensor based on vanadium dioxide (*Left*: the photograph of the VO_2 film-based breath sensor; *Right*: the resistance change of breath sensor during exhaling and inhaling). (B) Transferred TiO_2-nanofibers for protein detection from whole blood. (*Continued*)

Memristors have been considered promising candidates for next-generation memory and neuromorphic computing due to their remarkable advantages, such as simple structure, fast switching speed, and high energy efficiency. Cao et al. report Mg/MgO-based memristors with remarkable threshold switching behaviors and fully dissolvable characteristics and named physically transient memristors (Cao et al., 2022). Memristors are fabricated on a silicon substrate and then transferred onto the biocompatible and biodegradable PVA substrate to acquire the fully transient system. Memristor devices demonstrated the critical synaptic functions including paired-pulse facilitation, paired-pulse depression, and the transition from short-term to long-term plasticity. These functions can be attributed to the drift and diffusion of Mg^{2+} ions in the MgO resistive switching layer. Memristor could be degraded and dissolved in deionized water at room temperature, showing transient behaviors. We can conclude that physically transient memristors can be potentially applied in biodegradable or biointegrated neuromorphic computing systems, secure electronic devices, and green electronics.

A thin-film transistor (TFT) as a special type of field-effect transistor (FET) is thin relative to the conventional bulk metal oxide field effect transistor, which makes TFT to be an ideal candidate for fabricating flexible electronics. The fabrication of TFTs on flexible substrates is a key technique to realizing flexible electronics. It has attracted intensive research interest in recent years to fabricate TFT by using a-IGZO (amorphous indium-gallium-zinc oxide) as the key semiconductor. Compared to traditional amorphous silicon (a-Si), a-IGZO offers several attractive properties including optical transparency, high mobility, low-temperature deposition, and operational stability. Fig. 12.2C shows a schematic illustration of a-IGZO TFT and circuits formed on a Si wafer with a sacrificial Ni film (Jin et al., 2015). The a-IGZO TFT can be picked up by immersion in water and then transferred onto a flexible substrate for obtaining the flexible TFT. The electrical performances of flexible TFT, including field effect mobilities, on/off ratios, subthreshold slopes, and Ohmic contact properties, are all comparable to otherwise similar devices constructed in conventional ways. These characters show application possibilities in bioelectronics. Additionally, compared with synthetic polymers, biopolymers have ideal biocompatibility and similar mechanical properties to biotissue and are attractive bioelectronics substrate candidates. Collagen is one of the most extensively studied biopolymers. Collagen is an important component of the extracellular matrix and is found

(C) Thin film transistors and circuits based on amorphous indium − gallium − zinc oxide. (D) Fabricate the Zinc Oxide transistors on mammalian collagen. (E) Transferred silicon dioxide layers as biofluid barriers for biointegrated flexible electronic systems. *(A) Reproduced with permission; Copyright © 2007 IOP Publishing, Ltd; (B) Reproduced with permission; Copyright © 2015 The Royal Society of Chemistry Reproduced with permission; (C) Reproduced with permission; Copyright © 2015, American Chemical Society; (D) Reproduced with permission; Copyright © 2020 WILEY-VCH Verlag GmbH & Co. KgaA, Weinheim; (E) Copyright © 2016 National Academy of Sciences.*

in all tissues, particularly in connective tissues such as skin, tendons, corneas, and bone. However, denaturation temperature and swelling in water/vacuum have been fundamental barriers to the electronic fabrication of collagen. These problems can be avoided by transfer printing technology. As shown in Fig. 12.2D, flexible ZnO-based TFTs are fabricated on a carrier wafer (Si) using a sacrificial layer of germanium oxide and then transferred onto collagen (Moreno et al., 2020). The mobility and threshold voltage of the TFT on collagen shows only $\approx 41\%$ and $\approx 22\%$ drop compared to the ones on a rigid silicon substrate, which can be attributed to stresses experienced during the transfer, which may affect the gate/dielectric interface. These changes can be further reduced by optimizing the transfer process. Due to their high degree of biocompatibility, TFTs can be used for long-term implants.

Encapsulation materials are essential to the development of bioelectronics, especially for chronic electron implants. The encapsulation schemes for conventional electronic implants rely on thick (millimeter-scale), rigid enclosures constructed using bulk metal or ceramic parts, which is incompatible with the types of flexible bioelectronics. A challenge is in the development of materials that can serve as long-lived, perfect barriers to biofluids. This material should encapsulate the entire surfaces of the electronics, to prevent biofluid penetration across any exposed interfaces. Meanwhile, an encapsulation scheme is required to form high-quality sensing/actuating interfaces and compliant mechanical interfaces. Fig. 12.2E illustrates an encapsulation scheme: ultrathin, transferred layers of thermally grown silicon dioxide are used as biofluid barriers for flexible bioelectronic (Fang et al., 2016). The process begins with the thermal oxidation of a silicon wafer to form an ultrathin SiO_2 layer, and then high-quality functional electronics can be fabricated on this layer of oxide. The transfer process consists of bonding the top surface of this substrate onto a temporary supporting substrate. The silicon is removed by dry etching in a way that terminates at the bottom surface of the SiO_2. Peeling the device from the temporary support and yield a piece of flexible electronics encapsulated across its entire front surface with a layer of thermal SiO_2 as a barrier to biofluids. Similar growth and transfer processes can deliver a layer of SiO_2 to the bottom of the flexible substrate to prevent biofluid penetration from the back side. Accelerated lifetime tests suggest robust barrier characteristics on timescales that approach many decades, in layers that are sufficiently thin (less than 1 μm) to provide the compliant mechanical interface. Additionally, the bilayer barrier can offer more excellent capabilities to prevent water and ion permeation, such as HfO_2/SiO_2 barrier. Song et al. report that a 100/100-nm-thick bilayer of HfO_2/SiO_2 barrier has a lifetime ≈ 10 times longer than that of an isolated 100-nm-thick layer of thermal SiO_2 barrier. A bilayer of HfO_2 /SiO_2 barrier offers a projected lifetime of over 40 years at 37°C PBS (pH of 7.4) due to the enhanced ion-barrier properties, which shows the potential advantages for wide applications in chronic biointegrated devices.

12.2.3 Silicon

As a very important semiconductor material, Silicon (Si) plays a crucial role in our everyday lives. Silicon has broad applications in both electronic and photonic technologies and can be found in almost all electronic devices, including but not limited to laptops, smartphones, tablets, microwaves, and bioelectronics. The present microelectronics technology is based on silicon materials. They are also expected to play a more significant role in the next generation, such as flexible electronics. For conventional semiconductor materials and devices, there is a tradeoff between device performance and growth temperature, which is unreal for fabricating inorganic semiconductor materials on a flexible substrate due to poor thermo-chemical stability. The realization of electronics with performance equal to established technologies that use rigid semiconductor wafers, but in lightweight, foldable, and stretchable formats would enable many new applications (Fig. 12.3).

Various Si-based sensors are manufactured and integrated with flexible substrates, which have potential applications in the biomedical field. Kim et al. report an EES (Kim et al., 2011), which is achieve thicknesses, effective elastic moduli, bending stiffnesses, and areal mass densities matched to the epidermis, and thus is mechanically invisible to the user. By transferring printing technology, several classes of Si-based devices are integrated onto tattoo paper including Silicon MOSFET, silicon feedback resistor, Si solar cells, Si-based strain gauges, and Si PIN diode. EES is integrated with a collection of multifunctional sensors (such as temperature, strain, and electrophysiological), active/passive circuit elements (such as transistors, diodes, and resistors), wireless power coils, and devices for radio frequency (RF) communications (such as high-frequency inductors, capacitors, oscillators, and antennae). A key capability of EES is in monitoring electrical activity produced by the heart, brain, and skeletal muscles. As shown in Fig. 12.3A (Kim et al., 2011), the skin deforms freely and reversibly, without any apparent constraints in motion due to the EES. ECG recordings from the chest and EMG measured on the leg reveal high-quality signals. The measurements agree remarkably well with signals simultaneously collected using commercial, bulk tin electrodes, that require conductive gels, mounted with tapes at the same location. EES has potential applications in the biomedical field including physiological status monitoring, wound measurement/treatment, biological/chemical sensing, human-machine interfaces, covert communications, and others. Shin et al. report an optical pressure and temperature sensor that uses a Fabry-Pérotinterferometer (FPI) design (Shin et al., 2019). Fig. 12.3B upper photo shows a schematic illustration of an FPI pressure and temperature sensor composed of a thermally grown silicon dioxide (t-SiO_2) encapsulation layer, silicon nanomembranes (Si NMs), amorphous silica adhesion layer, and a slab of silicon with a square cavity. The layers of t-SiO_2 and Si NM serve as pressure-sensitive diaphragms that seal an air chamber formed by bonding with a silicon slab

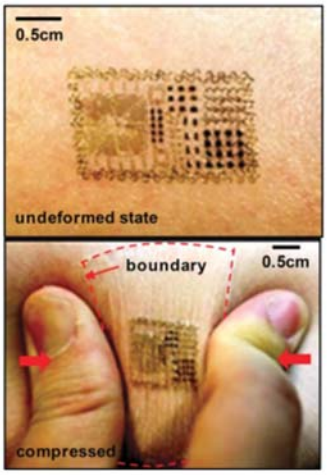

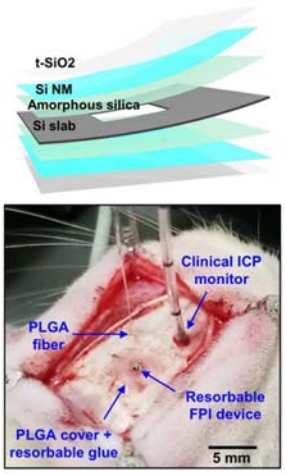

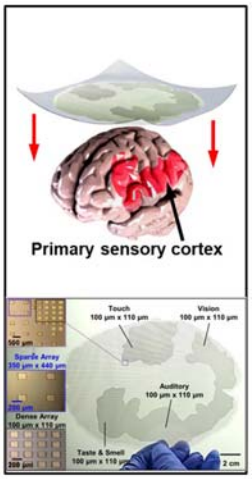

(A) (B) (C)

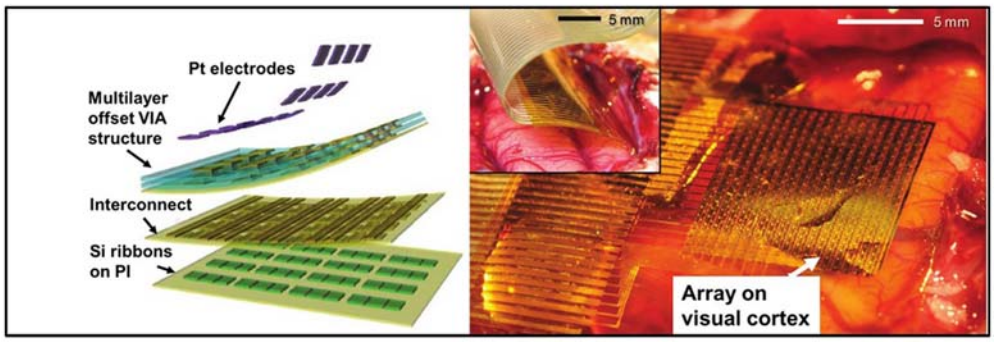

(D)

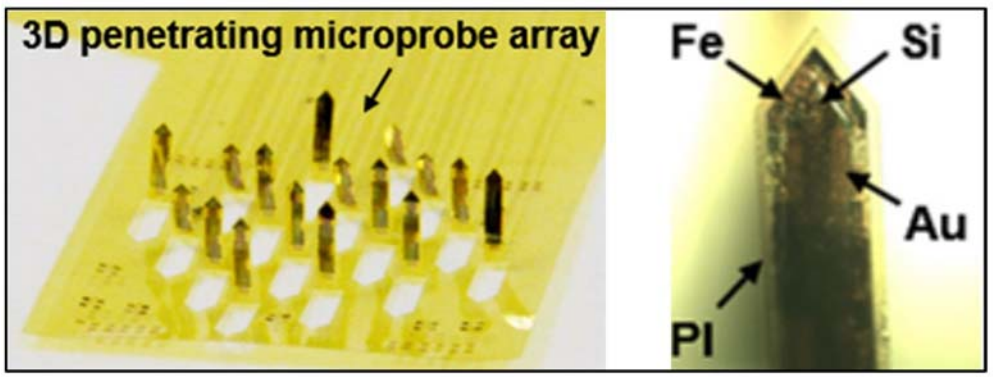

(E)

(*Continued*)

with a cavity. Optical fibers connected to a tunable laser and PD couple light in and out of the device to enable measurement of pressure and temperature via changes in measured reflection spectra. Sensors rely on pressure-induced deflections of Si NM diaphragms and the resulting changes in the thickness of an air cavity, which cause shifts in resonant peak positions in the reflection spectra. In vivo monitoring of intracranial pressure (ICP) and intracranial temperature (ICT) in rats demonstrates the potential clinical utility of these systems.

The transistor is the basic semiconductor device which uses for regulating the current and voltage in small electronic circuits. Transistors represent the fundamental device building blocks for microelectronics and are used in a wide variety of electronic devices. TFTs are well-compatible with flexible electronic systems due to compliant mechanical characteristics. As the most common active thin film devices, TFTs are significant building blocks for flexible platforms. Conventional Si-based TFTs are widely used in microelectronics. Flexible Si-based TFTs have been investigated for various amazing and unique applications. Viventi et al. report a class of mechanically flexible silicon electronics composed of 2016 silicon nanomembrane transistors for multiplexed measurement of signals in an intimate, conformal integrated mode on the dynamic, 3D surfaces of living biological tissues (Viventi et al., 2010). Benefiting from transfer printing technology, transistors integrated with flexible substrates show high performance. In vivo experiments are performed in male Yorkshire pigs. The flexible silicon electronics system is placed on the heart of an adult pig and conformed to the epicardial surface, including epicardial coronary vessels. The spread of spontaneous and paced ventricular depolarization with high temporal and spatial resolution is mapped using this electronic system. Large-scale electronic platforms that support intimate,

Figure 12.3 Si-based devices for wearable and implantable systems. (A) The multifunctional epidermal electronics based on Si-based electronics. (B) The Fabry-Pérot interferometer sensors for monitoring intracranial pressure and temperature (*Upper*: schematic illustration of an FPI pressure and temperature sensor; Bottom: the photograph of an FPI sensor implanted in the intracranial space of a rat). (C) Printed silicon microdie arrays with variable density for chronic biointegration (*Upper*: Schematic illustration of contact of the system on the surface of a brain model; *Bottom*: heterogeneous integration of Si microelectronics). (D) The flexible, high-density electrode array for mapping brain activity (*Left*: the schematic exploded view of each layer; *Right*: a flexible, high-density active electrode array was placed on the visual cortex). (E) The ultra-thin transfer printed Si optoelectronic microprobe arrays (*Left*: the optical image of microprobe array on a curved surface; *Right*: the optical microscopic image of a single microprobe). *(A) Reproduced with permission; Copyright © 2011, The American Association for the Advancement of Science; (B) Reproduced with permission; Copyright © 2019 The Authors, some rights reserved; exclusive licensee American Association for the Advancement of Science; (C) Reproduced with permission; Copyright © 2019 National Academy of Sciences; (D) Reproduced with permission; Copyright © 2011, Nature Publishing Group, a division of Macmillan Publishers Limited. All Rights Reserved; (E) Reproduced with permission; Copyright © 2018, The Author (s).*

functional biointerfaces offer important capabilities in monitoring and/or stimulation of living tissues. This platform can be potentially applied in neural recording. Fig. 12.3D left photo shows an electronic system that integrates ultrathin silicon nanomembrane transistors into the electrode array, enabling new dense arrays of thousands of amplified and multiplexed sensors that are connected using fewer wires (Viventi et al., 2011). This system is used to map neural activity at high resolution on the surface of the visual cortex of ten cats in vivo (as shown in Fig. 12.3D right photo). The electronic system can either sample broad regions of the brain at low spatial resolution or small regions of the brain at high spatial resolution. The electronic system can offer a spatial scale 400-fold finer than that used clinically (Viventi et al., 2011). The increases in spatial and temporal resolution would allow a more detailed characterization of brain networks. Song et al. establish a scalable approach for building combined electronic–optoelectronic microsystems that served as functional interfaces to soft tissues. As demonstrations, as many as tens of thousands ($>32{,}000$) of thin, microscale functional elements (including a pair of n-channel metal-oxide-semiconductor transistors) derived from source wafers are integrated with the flexible substrate by transferring printing method, as interconnected networks across areas that approach those of the human brain (as shown in Fig. 12.3C) (Song et al., 2019). The scalable approach may herald a new generation of diagnostic and therapeutic brain-machine interface devices.

With the rapid development of optogenetics, which optogenetics involves injecting light into the brain to stimulate or control neurons, the optical neural probe has attracted intensive research interest in recent years. Detecting the light intensity in spatial positions can facilitate the understanding of the biological consequences. Sim et al. report a penetrating microprobe array can serve this purpose. The 3D penetrating microprobe array is formed in a thin and flexible format, which can attach and conform to curved surfaces and whose function is enabled by transfer printed ultrathin Si PDs (Sim et al., 2018). The PD employs two n–p Si diodes configured in a back-to-back (n–p–p–n) fashion. Fig. 12.3E shows an optical image of a 3D penetrating microprobe array on a curved surface (left photo) and an optical microscopic image of a single microprobe (right photo) (Sim et al., 2018). The capability of mapping the photo intensity in space is verified in a brain model. This type of penetrating microprobe array can find potential and broad utilities in a wide range of biointegrated applications, such as optogenetics, deep brain stimulation, cortex mapping, etc.

12.2.4 Wide bandgap semiconductors

Si semiconductor technology is approaching the theoretical limits of the Si material. To overcome this limitation and fabricate high-performance devices, new semiconductor materials are needed. Wide bandgap semiconductors like silicon carbide (SiC),

gallium nitride (GaN), and diamond, due to their superior electrical characters are likely candidates to replace Si shortly for high power, or high frequency, and short wavelength optoelectronic devices. Among these, diamond is an attractive material due to its exceptional physical characteristics, including the hardest materials, high density, the highest thermal conductivity, optical transparency that extends from the far infrared to the deep ultraviolet, low coefficient of thermal expansion, chemically inert, and excellent biological compatibility. Using the transfer printing method, many flexible diamond-based devices emerge for application in the biomedical field. Hess et al. report a chemical release transfer method to integrate microcrystalline diamond film onto a mechanically flexible polymer substrate (Hess et al., 2011). The high-temperature diamond growth process is performed on a temperature-tolerant substrate (Si wafer) using a thin SiO_2 film as a sacrificial layer, and then the diamond film is released from the wafer by dissolving the SiO_2 sacrificial layer in HF, thus transferring the diamond film from the Si/SiO_2 wafer to the flexible polymer substrate. The flexibility of the diamond-on-polymer structure is confirmed by wrapping the dogbone-shaped test structure around a cylindrical object with a radius of 650 μm without resulting in diamond delamination or cracking. The diamond-on-polymer structures can withstand a high degree of bending around small radii of curvature and will be able to conform well to curved biological structures (Fig. 12.4).

In addition to electrical and mechanical properties, biocompatibility is essential for bioelectronic devices, especially for implantable devices. Critical to the success of bioelectronics is reducing the immune response of an organism to the external device. Ideally, an implant is biologically inert and does not activate an immunological response but allows target cells to integrate with the bioelectronic application. If the bioelectronic device elicits an immunological response, the device may become encapsulated within a fibrous tissue, compromising or seriously disrupting the interface between the device and neural tissue (Feron et al., 2018). Bendali et al. develop a procedure for depositing diamond onto flexible 3D retinal implants (shown in Fig. 12.4A upper photo) and investigate the biocompatibility of diamond as an electrode (Bendali et al., 2015). In vitro experiment shows diamond electrode displays biocompatibility with embryonic cortical neurons and stem cells and even retinal neurons. For investigation of the biocompatibility of diamond in vivo, soft polyimide implants with diamond are inserted into the subretinal space of P23H rats (shown in Fig. 12.4A bottom photo). The absence of a massive inflammatory reaction and the presence of many bipolar neurons suggest that diamond electrodes are not toxic to retinal neurons. This study confirms the considerable benefits of the diamond as an attractive electrode material applicated in the biomedical field. Additionally, diamond is favorable material for biochemical sensors due to it has biocompatibility, chemical inertness, resistance to biofouling, extremely wide potential window, and low double-layer capacitance. Fig. 12.4B shows flexible, diamond-based microelectrodes for neural sensing, which

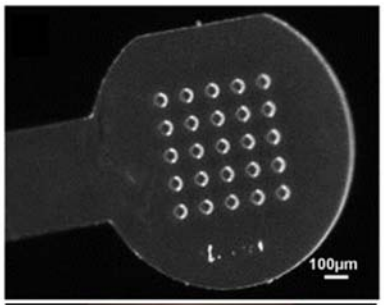

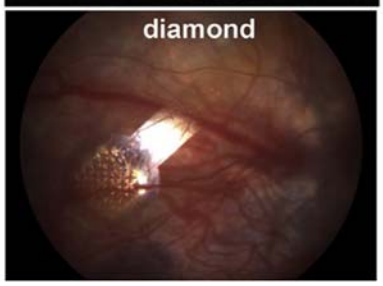

(A)

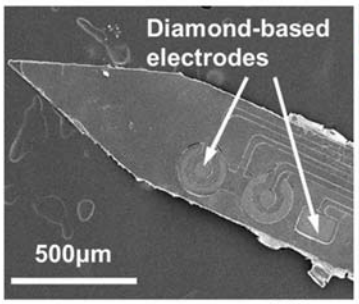

(B)

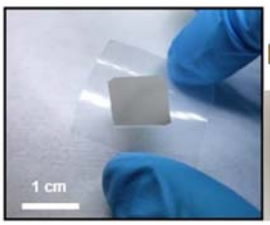

(C)

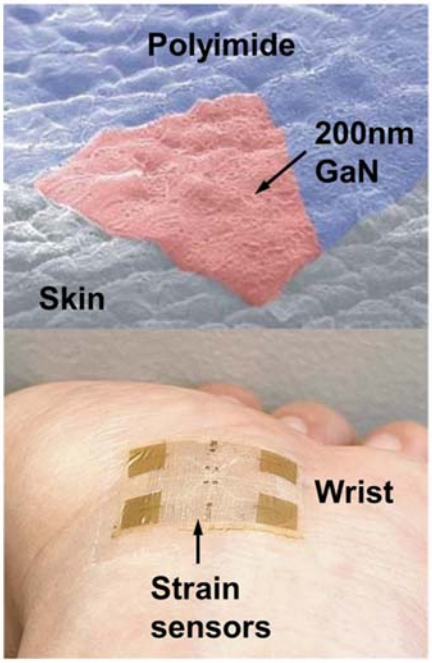

(D)

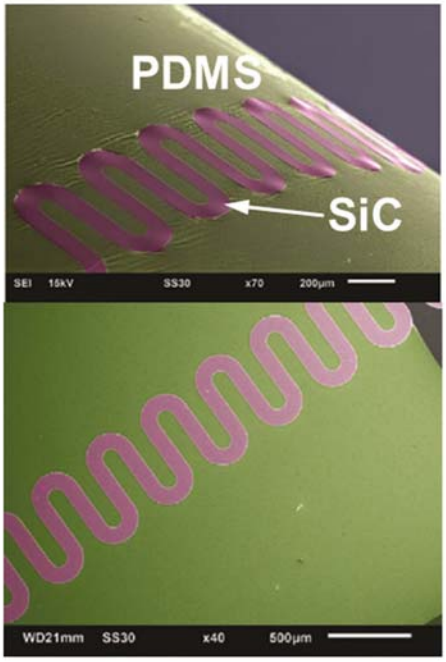

(E)

(*Continued*)

consist of multichannel boron-doped polycrystalline diamond (BDD) microelectrodes on a soft Parylene C substrate (Fan et al., 2020). The dopamine (DA) sensing capability of the BDD microelectrodes is validated in a 1.0 mM dopamine solution. The BDD microelectrodes exhibit a featureless background current and wider water potential windows compared to the standard gold electrode, which permits the detection of chemical analytes in an expanded potential range of operation with reduced interference from the non-Faradaic background current of the electrolyte.

Despite its unique features, the wide application of diamond in the biomedical field is limited by processing technologies and difficulties in its integration with heterogeneous devices and substrates. Xie et al. report a facile process to form large-area, free-standing diamond thin films and combine them with optoelectronic devices on flexible substrates. By transferring printing, diamond thin films released from original substrates can be heterogeneously integrated onto any foreign substrates of interest. As shown in Fig. 12.4C left photo, diamond thin films are transferred onto a polyethylene terephthalate (PET) substrate (Xie et al., 2021). Diamond films are heterogeneously integrated with micro-LEDs to facilitate heat dissipation during operation (shown in Fig. 12.4C right photo). Experimental and calculation results suggest that the temperature rises during operation for micro-LEDs can be reduced by approximately 20% by using diamond films as heat sinkers. These materials and device strategies provide promising paths to the broad applications of thin-film diamonds in the biomedical field.

As the representatives of the wide band gap semiconductor materials, GaN has been widely studied due to their excellent characteristics and plays an important role in solid-state lighting, flat panel displays, solar energy, electronic power, and other

Figure 12.4 Wide bandgap materials. (A) Three-dimensional (3D) diamond-based electrodes for flexible retinal neuroprostheses (*Upper*: SEM image of 3D diamond-based electrodes; Bottom: eye fundus of rat with implanted diamond-based electrodes). (B) Flexible diamond-based microelectrodes for neural sensing (*Left*: SEM images of a fabricated implantable neural probe; *Right*: setup of in vivo neural recording in a male rat). (C) Biocompatible diamond thin films integrated with flexible substrates (Upper: the free-standing diamond films on PET-based flexible substrates; *Bottom*: the schematics and corresponding images of diamond films integrated with blue micro-LEDs). (D) The wireless e-skin based on freestanding ultrathin single crystalline GaN film (*Upper*: SEM images of GaN e-skins with 200-nm-thick GaN attached to skin replica samples; *Bottom*: the wireless pulse measurements using GaN e-skin strain sensors). (E) The freestanding SiC for implantable and stretchable bioelectronics (*Upper*: SEM images of the SiC spring/PDMS membrane under mechanical deformation; *Bottom*: SEM images of the free-standing SiC micro-spring structures). *(A) Reproduced with permission; Copyright © 2015 Published by Elsevier Ltd.; (B) Reproduced with permission; Copyright © 2020 The Author (s); (C) Reproduced with permission; Copyright © 2020 Wiley-VCH GmbH). (D) Reproduced with permission; Copyright © 2022 The American Association for the Advancement of Science; (E) Reproduced with permission; Copyright © 2021 IOP Publishing Ltd Printed in the UK.*

fields. GaN also has great potential applications in bioelectronics. Kim et al. report a chipless wireless e-skin based on surface acoustic wave sensors made of freestanding ultrathin single-crystalline piezoelectric GaN membranes. The ultrathin GaN epitaxial layers (200 nm) are grown on graphene (GP)-coated GaN substrates and are easily released from the weak GP−GaN interface. Then ultrathin GaN films are transferred on a flexible patch as the material for passive wireless sensing. The excellent piezoelectricity and perfect single-crystallinity of GaN film enable wireless communication without chips. As shown in Fig. 12.4D upper photo, ultrathin GaN films can conformal coverage on the skin replica made of Ecoflex silicone (Kim et al., 2022). The chipless wireless e-skin allows the continuous measurement of arterial pulse waves on the wrist with highly sensitive over 7 days (as shown in Fig. 12.4D bottom photo). This presents routes to inexpensive, high-sensitivity platforms for wireless health monitoring devices.

SiC is an attractive candidate for bioelectronic devices among various wide bandgap semiconductor materials due to its chemical inertness and stable mechanical and electrical properties and is suitable for integration in reliable implantable, and stretchable sensing devices. Pham et al. report a versatile transfer printing process that employs a thin aluminum film as a sacrificial layer to facilitate the release and transfer diverse SiC films from rigid Si wafers onto flexible PDMS substrates (shown in Fig. 12.4E) (Pham et al., 2020). The transferred SiC films exhibit a high degree of structural perfection without cracks or tears and good semiconducting functionality. The SiC surface is an inert, nontoxic contact site that allows cells to firmly attach, proliferate, and then eventually spread to establish cell−cell contact. The physiological and morphological features of the human dermal fibroblast on the SiC surface are investigated. The results indicate the cytological compatibility of SiC and demonstrate the potential of flexible SiC electronics for implantable applications.

12.2.5 Two-dimensional materials

2D materials are emerging material candidates for electronic and photoelectric devices, energy storage, conversion devices, and bioelectronics. The most fascinating feature of 2D materials is their ultrathin vertically layered nanostructure that provides high optical transparency, extraordinary softness, and inherent flexibility to the devices. The quantum confinement effect in atomically thin layered nanostructure also introduces interesting optoelectronic characteristics and superb photodetection capabilities. The large-area continuous planar structure of 2D materials allows efficient carrier transport within the 2D plane. Benefiting from the unique 2D layered structure and outstanding properties, 2D materials have proven to be good candidates for flexible bioelectronic devices. These interesting properties of the 2D materials enable unconventional device functions in biological and optical sensing, as well as superb performance in electrical and biochemical therapeutic (Choi et al., 2019) (Fig. 12.5).

Among various 2D materials, GP stands out in the flexible electronics field due to its combination of high carrier mobility, high thermal conductivity, high specific surface area, high optical transparency, excellent mechanical flexibility, and environmental stability. GP is an ideal material for wearable and implantable electronics. Lim et al. report a transparent and stretchable interactive human−machine interface (iHMI) system composed of wearable motion sensors which consist of piezoelectric polymer (PLA)/SWNT composite thin film sandwiched between GP electrodes and insulating layers (shown in Fig. 12.5A upper photo) (Lim et al., 2015). The GP is grown through a chemical vapor deposition (CVD) process using copper as the catalyst and transferred onto the top and bottom surfaces of PLA/SWNT composite thin film respectively to form sandwich structures. The bending tests confirm that GP heterostructures maintain their high electrical conductivity even after being subjected to extreme bending. The iHMI system can be conformally laminated onto human skin (shown in Fig. 12.5A bottom photo) and have a natural appearance, comfort, and high SNR, which benefits from the high conductivity of GP and the ultrathin and lightweight design.

GP is an emerging ideal transparent electrode material due to high optical transparency and high electrical conductivity. GP biocompatibility increases its potential use in implantable biomedical applications. Fig. 12.5B shows a transparent and flexible low-noise GP electrode, which enables simultaneous optical imaging and electrophysiological recording (Kuzum et al., 2014). CVD-grown GP on Cu substrate is transferred onto the desired areas of the polyimide substrate using the poly(methyl methacrylate) (PMMA)/PDMS stamping method and is patterned using photolithography and oxygen plasma etching. In vivo experiments confirm that transparent GP electrodes can simultaneously record neural activity during calcium imaging with confocal or multiphoton microscopy without any light-induced artifacts in the electrical recordings. GP transparent electrodes offer a solution for high spatial-temporal resolution electro-optic mapping of the dynamic neuronal activity.

GP as a promising electrode material has tremendous potential for electrochemical sensing and biosensing due to excellent properties including chemical inertness, high conductivity and electron mobility at room temperature, large surface-to-volume ratio, and robust mechanical and flexibility. Mannoor et al. establish an approach to integrate GP electrochemical electrodes with biomaterials. The CVD-grown GP thin films are released from donor substrate and transferred onto the silk films. Planar inductive and capacitive elements are then incorporated onto the GP/silk samples to enable wireless interrogation (shown in Fig. 12.5C left photo) (Mannoor et al., 2012). GP-based sensing element with wireless readout coil is then transferred onto biomaterials via dissolution of the supporting silk film (shown in Fig. 12.5C right photo). The sensor is integrated onto the surface of a bovine tooth for investigating the performance (shown in Fig. 12.5C right photo). The results exhibit the capability of remote monitoring of pathogenic bacteria.

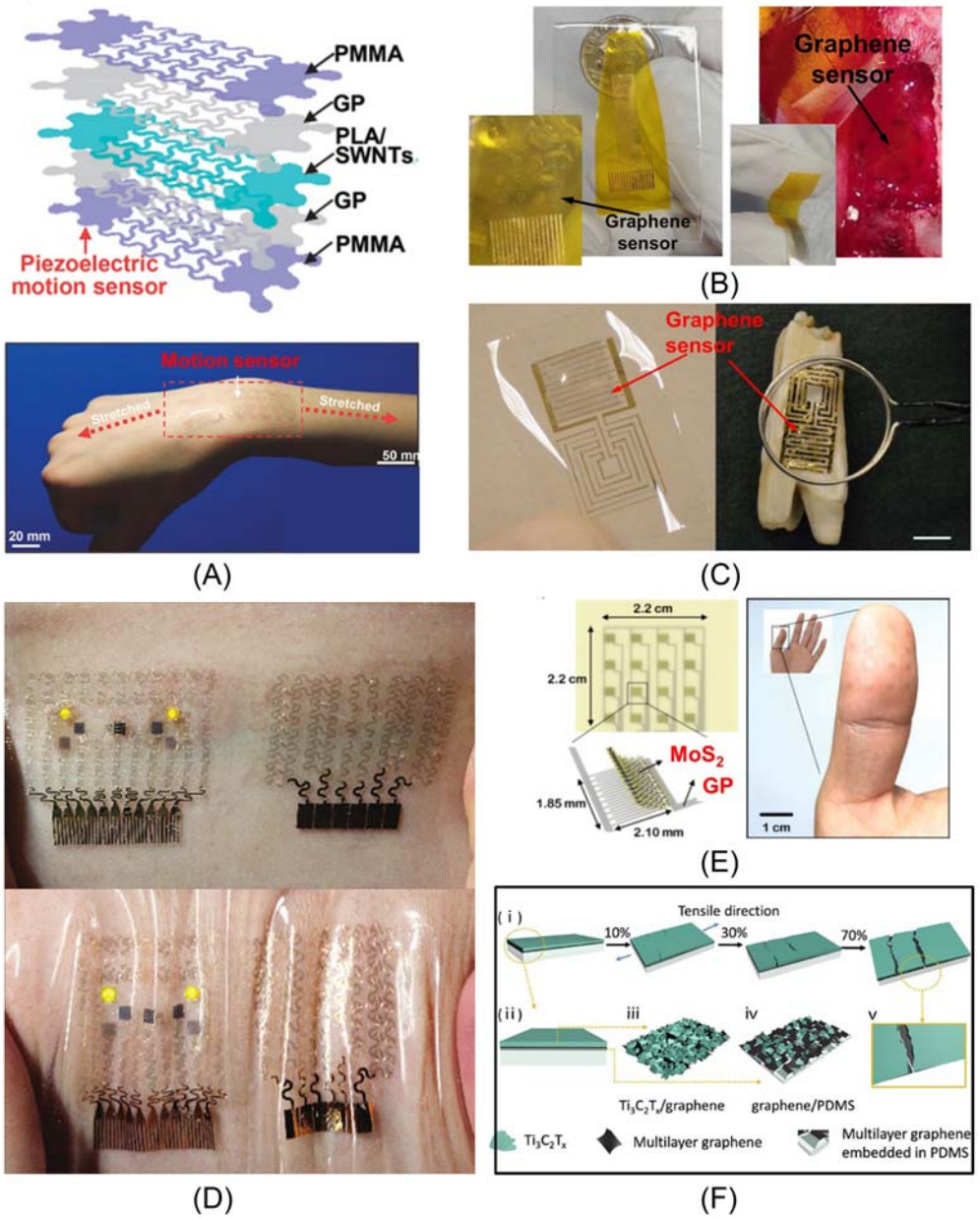

Figure 12.5 Two-dimensional (2D) materials. (A) Transparent and stretchable interactive human-machine interface based on transferred graphene (*Upper*: the exploded schematics of the transferred graphene used in the motion sensor; *Bottom*: the image of the motion sensor on the human wrist). (B) Graphene electrodes for simultaneous electrophysiology and neuroimaging (*Left*: the

(*Continued*)

However, the low defect density of CVD-grown GP results in poor electrochemical activity, which limits its application in biosensing. To overcome this limitation, gold-doped GP is used to replace GP for electrochemical sensing. Lee et al. report that GP doped with gold and combined with a gold mesh has improved electrochemical activity over bare GP and fabricate a stretchable patch for sweat-based diabetes monitoring (Lee et al., 2016). The gold mesh and gold-doped GP form an efficient electrochemical interface for the stable transfer of electrical signals. The patch with stretchable designs shows extremely conformal contacts to the human skin under deformation (shown in Fig. 12.5D). This conformal and intimate interfacing enables stable sensing.

MoS_2 materials have recently attracted attention due to their outstanding mechanical and optical transmittance, high gage factor, and tunable band gap. Fig. 12.5E shows an ultrathin conformal, MoS_2-based tactile sensing array (Park et al., 2016). Bilayer MoS_2 (1.4 nm) used as a strain-sensing layer is transferred on SU-8 substrate (32 nm). Transferred GP (0.9 nm) is used as an electrode. The total thickness of the sensor is less than 75 nm. The ultrathin tactile sensor shows high sensitivity, good uniformity, and linearity. In addition, it provides excellent mechanical flexibility, good optical transparency, and stable performance even on a human fingertip (shown in Fig. 12.5E right photo).

Laser-induced graphene (LIG) is a 3D porous material prepared by direct laser writing with a CO_2 laser on carbon materials in ambient atmosphere (Ye et al., 2019). This technique combines 3D GP preparation and patterning into a single step without the need for high-temperature reaction conditions, solvent, or subsequent treatments. Since its discovery in 2014, LIG has attracted broad research interest (Lin et al., 2014; Ye et al., 2018). Using transfer printing technology, LIG could integrate with various substrates and obtain exciting performance. He et al. report a self-healable, flexible, and multimodal sweat sensor based on LIG electrodes for healthcare monitoring

photograph of a 16-electrode array; *Right*: the photograph of the graphene electrode placed on the cortical surface of the left hemisphere of rat). (C) Graphene-based wireless bacteria detection platform. (D) Graphene-based electrochemical device for glucose monitoring (*Upper*: the optical image of the electrochemical sensor array; *Bottom*: the optical images of electrochemical sensor array on human skin). (E) MoS2-based tactile sensor for electronic skin applications (*Left*: the fabrication steps for the strain gage sensor based on the MoS2; *Right*: the photographs of the MoS2 tactile sensor on a fingertip). (F) Wearable strain sensors based on transferred MXene-graphene composite materials. *(A) Reproduced with permission; Copyright © 2014 WILEY-VCH Verlag GmbH & Co. KGaA, Weinheim; (B) Reproduced with permission; Copyright © 2014, Nature Publishing Group, a division of Macmillan Publishers Limited. All Rights Reserved; (C) Reproduced with permission; Copyright © 2016, Nature Publishing Group; (D) Reproduced with permission; Copyright © 2012, Nature Publishing Group, a division of Macmillan Publishers Limited. All Rights Reserved; (E) Reproduced with permission; © 2016 WILEY-VCH Verlag GmbH & Co. KGaA, Weinheim Reproduced with permission; Copyright © 2019 Elsevier Ltd. All rights reserved.*

applications, which can conduct simultaneous detections of pH, UA, and Tyrosine in sweat (He et al., 2021). The LIG on the donor substrate is pressed onto the self-healing substrate. Due to the strong adhesive force provided by the hydrogen bonds in the self-healing elastomer, the patterned LIG is thus transferred from the donor substrate onto the self-healing substrate. Due to the highly porous structure and high electron mobility of LIG, the sensor has outperformed commercial glassy carbon electrodes in terms of sensitivity to the targeted uric acid and tyrosine molecules. In addition, the sensor can recover from catastrophic through-cut damage by a razor blade, which benefits from the self-healable substrate.

Due to high metallic conductivity, good oxidation resistance, and excellent mechanical properties, MXenes have been integrated with various flexible substrates for bioelectronic applications (Li et al., 2019; Yang et al., 2019; Zhan et al., 2020). Sun et al. report a wearable strain sensor based on a spontaneously formed $Ti_3C_2T_x$/graphene/PDMS layered structure, which requires no complicated manufacturing process (Yang et al., 2019). As shown in Fig. 12.5F, a $Ti_3C_2T_x$ suspension prepared by a chemical liquid etching method and a multilayer GP suspension prepared by an electrochemical exfoliation method is mixed and filtrated into a conductive film. Then the $Ti_3C_2T_x$/GP films are transferred to prepolymerized PDMS substrates to form flexible and stretchable strain sensors. The strain sensor can be divided into two layers when being stretched: a $Ti_3C_2T_x$ dominated brittle upper layer and a flexible GP/PDMS composite bottom layer. The upper layer is brittle and tended to generate cracks to dissipate stresses when being stretched, while the bottom layer kept contact to maintain the conductive pathways. The synergetic motion of the upper and bottom layers rendered the film with highly sensitive and linear responses to strains in a wide strain range.

12.2.6 Biomaterials

Applications in biotechnology demand the ability to pattern relevant bioorganic materials, ranging from small molecule drug candidates to living cells (Carlson et al., 2012). The transfer printing technique is available for such purposes. It has been verified that various biomaterials can be patterned using the transfer printing method, such as DNA, proteins, Viruses, and cell. DNA patterned has become one of the essential tools to investigate the expression or mutation of thousands of genes simultaneously. Fig. 12.6A shows a simple and cost-effective transfer scheme for patterning DNA with high submicron resolution (Thibault et al., 2005), which is named namely microcontact printing. The patterned stamps are made of elastomeric poly (dimethylsiloxane) (PDMS) which has a strong hydrophobic surface and does not require any surface modification to be able to adsorb oligonucleotides or PCR products. The adsorbed DNA molecules are subsequently printed efficiently on a target surface. Experiments confirm

that this scheme can pattern DNA microarrays at a relatively high speed, high resolution, and high reproducibility (Thibault et al., 2005). DNA patterns can also be replicated at large-scale high resolution by other forms of printing, such as supramolecular nanostamping (SuNS) (Yu et al., 2005; Yu & Stellacci, 2006) and liquid supramolecular nanostamping (LiSuNS) (Yu & Stellacci, 2007). Supramolecular nanostamping encompasses a class of protocols that form high-resolution patterns of single-stranded DNA molecules. Additionally, LiSuNS and SuNS have a common advantage: the ability of printing features made of different DNA sequences in a single printing cycle while preserving their chemical differences (shown in Fig. 12.6B) (Yu & Stellacci, 2007) (Fig. 12.6).

Microcontact printing technology can also be used for patterning proteins. As shown in Fig. 12.6C. Renault et al. propose modified microcontact printing: patterning stamp surfaces with ensembles of biomolecules where the pattern on the affinity stamp is determined by the position of various proteins covalently linked to a planar stamp (Renault et al., 2002). After the capture process, target protein molecules are patterned on the stamp, and can be microcontact-printed onto a substrate in one step. This method enables the simultaneous capture of different target proteins from a complex solution (shown in Fig. 12.6C). Wigenius et al. report a simple method based on PDMS stamps can be used to pattern proteins: hydrophobic patterns achieved by transfer printing silicone oligomers from a PDMS stamp onto a hydrophilic substrate can selective adsorption of proteins from solution (shown in Fig. 12.6D) (Wigenius et al., 2008).

Additionally, the subtractive printing technique has been developed as a versatile method for the patterned transfer of proteins and viruses from solution to substrate through a series of step-wise reductions in nonspecific hydrophobic interactions. This method can be used to generate patterns with sub-100 nm resolution (Coyer et al., 2007; Solis et al., 2010). Fig. 12.6E shows the nanometer-scale patterning of viruses (M13 bacteriophages) by subtractive printing (Solis et al., 2010). A planar, hydrophobic elastomer (PDMS) using the spontaneous adsorption of viruses from solution onto hydrophobic surfaces, to subtract viruses from the elastomer using a nanotemplate during a brief contact step, and to print the remaining viruses pattern from the elastomer onto the target substrate. The key in this method is that the nano-template and final substrate have a higher work of adhesion for water than the elastomer.

Cell patterning in two and three dimensions provides great opportunities for basic science investigations, tissue engineering, and regenerative medicine applications (Schiele et al., 2010). Transfer printing technology can enable precise cell placement on 2D and even 3D surfaces. Stevens et al. report a simple potentially generic methodology for generating patterns of mammalian cells on porous scaffolds (Stevens et al., 2005). The hydrogel stamps are used in this method, which provided a "wet," biocompatible surface and maintained the viability of cells adsorbed on stamps during the patterning process.

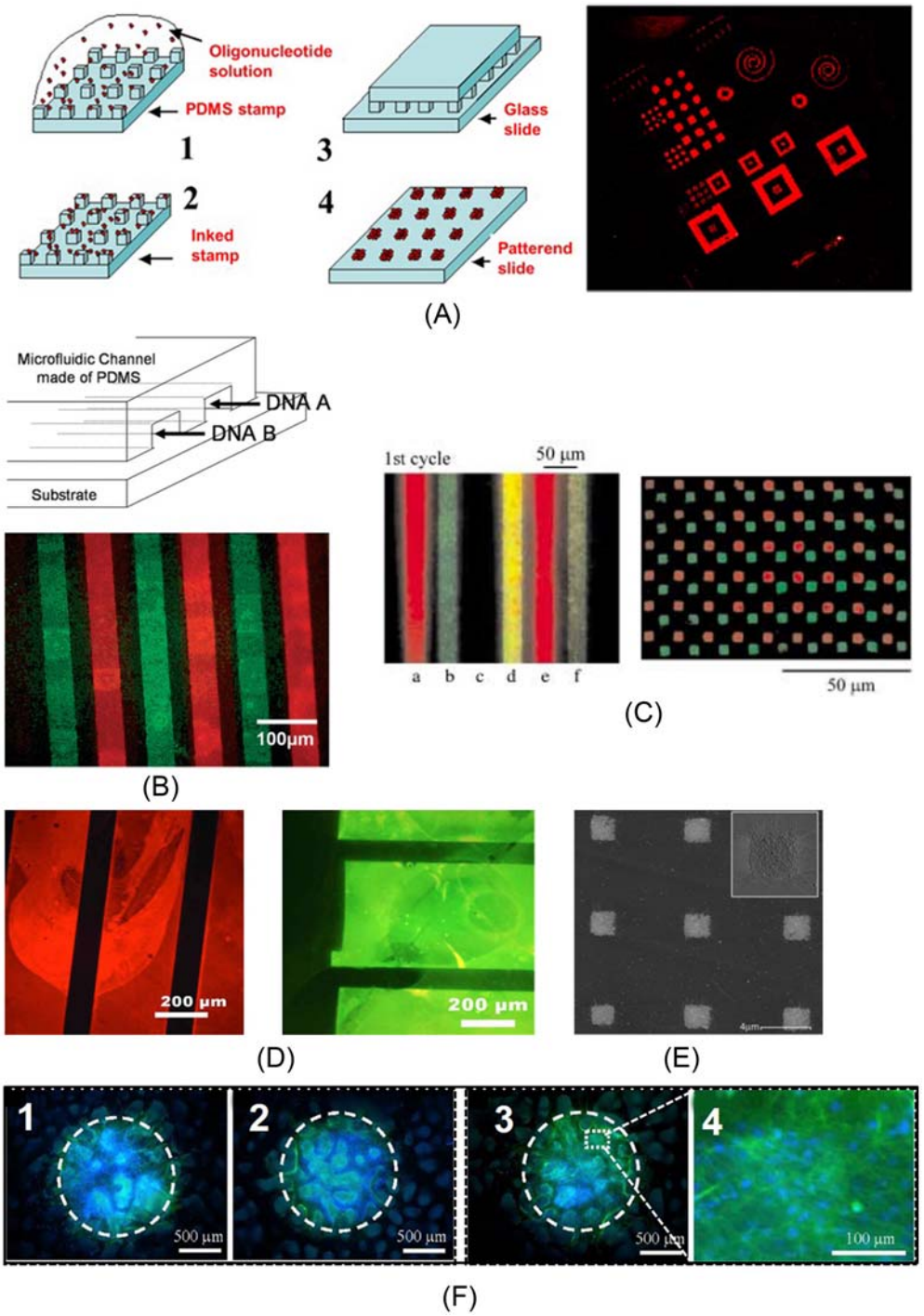

Figure 12.6 Biomaterials. (A) Transfer printing of oligonucleotides for biochip applications (*Left*: the principle of microcontact printing of DNA molecules; *Right*: the fluorescence images of printed micronic patterns). (B) Large-area transfer printing DNA via liquid supramolecular nanostramping (*Continued*)

The technique transferred material to the surface of the substrate in parallel, making it possible to pattern multiple spots of cells simultaneously. Fig. 12.6F shows three spots of cells patterned on the surface of hydroxyapatite at the same time and illustrates the reproducibility of the pattern transfer.

12.3 Functional devices

12.3.1 Light emitting diodes

LEDs have received considerable attention as a new light source in biomedical fields due to their high efficiency, long life, low power consumption, excellent portability, and easy integration with other electronic devices (Corbett et al., 2017; Zhang, Peng, et al., 2022). In addition to common phototherapy, their applications have been expanded to optical neural modulation, photodynamic therapy, and optical sourcing (Gutruf & Rogers, 2018; Lee et al., 2012; Lee et al., 2022). With the rapid development of optogenetics, micro-LEDs as implantable optical sources for controlling neurons have attracted intensive research interest in recent years. The implantable LED optical sources can provide precision optical stimulation, effective photon treatment, and other benefits. By integrating the micro-LEDs with flexible substrates, biocompatibility at the chemistry and mechanics level can be obtained, which are critical specifications for the long-term integration of implants with a biological host (Fallegger et al., 1903). Li et al. report a heterogeneous integration strategy, which enables the integration of tri-color (red, green, and blue) microscale, thin-film LEDs with the heterogeneous substrate (Li, Tang, et al., 2021). The first and key step

(*Upper*: the schematic illustrating the approach used for master preparation; *Bottom*: a false-color overlay of printed result). (C) Fabricating high-resolution arrays of proteins via affinity contact printing (*Left*: the captured molecules on the stamp are chicken IgGs (lines a and e), goat IgGs (lines b and f), protein A (line d), and mouse IgGs (line c); *Right*: the fluorescence microscope image showing the placement of the TRITC-anti-chicken and FITCanti-goat antibodies from a stamp onto a glass substrate). (D) Protein biochips patterned by microcontact printing [the fluorescence microscopy pictures of aIgG-Alexa μCP onto glass substrates followed by incubation with IgG-TxR illuminated at 546 nm (*left*) and followed by incubation with streptavidin-FITC illuminated at 470 nm (*right*)]. (E) The patterned transfer of viruses from solution to the substrate. (F) Mammalian cells are transferred onto porous tissue engineering substrates by hydrogel stamps (images 1−3 show different regions of a hydroxyapatite scaffold patterned with osteoblasts using a single agarose stamp; 4 is the higher magnification of the area within the white box in 3). *(A) Reproduced with permission; Copyright © 2005, Thibault et al.; licensee BioMed Central Ltd.; (B) Reproduced with permission; Copyright © 2007 WILEY-VCH Verlag GmbH & Co. KgaA, Weinheim; (C) Reproduced with permission; Copyright © 2002 WILEY-VCH Verlag GmbH, Weinheim, Fed. Rep. of Germany; (D) Reproduced with permission; Rights managed by AIP Publishing; (E) Reproduced with permission; Copyright © 2010 WILEY-VCH Verlag GmbH & Co. KGaA, Weinheim; (F) Reproduced with permission; Copyright © 2005 Elsevier Ltd. All rights reserved.*

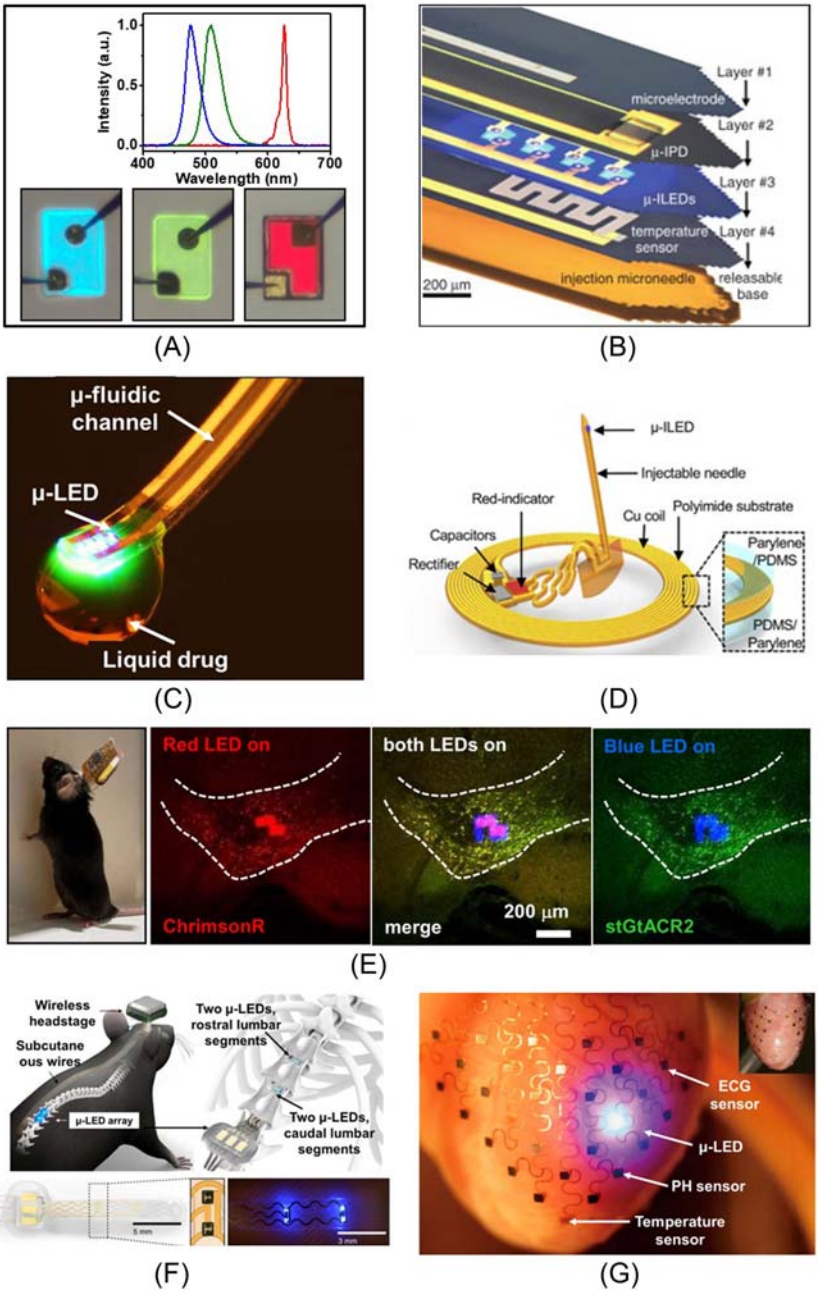

Figure 12.7 Microlight emitting diodes (LEDs) for implantable light sources. (A) Microscope images and electroluminescence spectra of multicolor micro-LEDs after transfer printing. (B) GaN μ-LEDs are transferred onto thin plastic strips for optogenetics. (C) Optofluidic neural probes that combine

(*Continued*)

in this integration strategy is forming free-standing thin-film LEDs. Thin-film, freestanding red LEDs based on gallium arsenide (GaAs) are formed by selective sacrificial etching: a lattice-matched $Al_{0.95}Ga_{0.05}As$ sacrificial layer is incorporated beneath the epitaxial layer during the growth of functional structure, and then thin-film LEDs can be released from the grown substrate by highly selective etching of sacrificial layer. Thin-film GaN-based blue/green LEDs are released from sapphire by a laser lift-off (LLO) technique. Free-standing LEDs can be integrated with various foreign substrates, such as flexible, stretchable, and even biodegradable substrates. Fig. 12.7A shows the Microscope images and spectrum of tri-color (red, green, and blue) thin-film LEDs integrated with the flexible substrate. This integration strategy enables a wide range of new opportunities for fabricating a multifunctional flexible optogenetic platform with good biocompatibility and conformability (Li et al., 2021). Fig. 12.7B shows a multifunctional optogenetic probe consisting of micro-LEDs to enable optical stimulation, precision temperature sensors to monitor thermal load, platinum microelectrodes to perform electrical recording, and a micro-scale PD to allow for photometry (Kim et al., 2013). Despite its multilayer structure, the multifunctional optoelectronic systems have a total thickness of approximately $\sim 20\ \mu m$, high mechanical flexibility, and minimally invasive stimulation. Another example is Fig. 12.7C shows optofluidic neural probes consisting of soft microfluidic drug delivery with micro-LED arrays, which enable programmed spatiotemporal control of fluid delivery and photostimulation (Jeong et al., 2015). The microfluidic channel is fabricated by bonding two transparent thin elastomers (PDMS), which enable high flexibility and transmittance after incorporation with μ-LED arrays. Experiments in freely moving animals demonstrate that the dopaminergic system is activated by micro-LED, and then blocked by dopamine receptor antagonists delivered through the microfluidic channel in a temporally precise programmable manner. Conventional hardware for optogenetic stimulation physically tethers the experimental animal to an external power supply equipment

soft microfluidic drug delivery with micro-LED arrays. (D) Flexible near-field wireless optogenetic probe. (E) Dual-color optogenetic probe for simultaneous neural activation and inhibition in the same brain region (*Left*: the photograph of a behaving mouse after intracranial implantation of a probe; *Right*: micrographs of a dual-color micro-LED probe embedded into the tissue). (F) Closed-loop optogenetic probe across the entire dorsoventral spinal cord (Upper: the schematic overview of the optoelectronic; Bottom: photographs of the micro-LED array). (G) Micro-LEDs are served as local light sources in a 3D multifunctional integumentary membrane integrated on a rabbit heart (Inset: the electronics can cover both anterior and posterior surfaces of the heart). *(A and B) Reproduced with permission; Copyright © 2013, The American Association for the Advancement of Science; (C) Reproduced with permission; Copyright © 2015 Elsevier Inc. All rights reserved; (D) Reproduced with permission; Copyright © 2016 Elsevier Inc; € Reproduced with permission; Copyright © 2022, The Author (s); (F) Reproduced with permission; Copyright © 2021, The Author (s), under exclusive license to Springer Nature America, Inc.; (G) Reproduced with permission; Copyright © 2014, Nature Publishing Group, a division of Macmillan Publishers Limited. All Rights Reserved.*

and imposes constraints on the animal's movement. Emerging wireless options offer important capabilities to solve this problem. Fig. 12.7D shows a thin, flexible, and fully implantable wireless optogenetic system, which combines subdermal magnetic coil antennas connected to micro-LEDs (Shin et al., 2017). This wireless system can operate at wavelengths ranging from UV to blue, green-yellow, and red. This wireless power transfer technology has a low operating frequency (13.56 MH), which reduces the absorption in biological tissues, provides greater penetration depth, and minimizes adverse biological effects (Fig. 12.7).

To control neural activities more precisely, bidirectional neural modulations are required. Li et al. report a wireless dual-color optogenetic probe, which comprises vertically integrated microscale thin-film red and blue LEDs and exhibits superior biocompatibility for long-term light stimulation in vivo (Li, Lu, et al., 2022). Cooperating with the coexpression of two spectrally distinct excitatory and inhibitory channelrhodopsins (ChrimsonR and stGtACR2), bidirectional optogenetic activation and inhibition are achieved in behaving mice. In vivo experiment results demonstrate that wireless dual-color optogenetic probes enable efficient, bidirectional control of neuronal activity in the ventral tegmental area and dopamine release of the nucleus accumbens (shown in Fig. 12.7E). These technologies provide numerous opportunities and implications for neuroscience research.

Photogenetic, as an efficient neural modulation technology, enables millisecond-scale optical control of neural activity in defined cell types during animal behavior, which allows scientists to pursue closed-loop optogenetic control (Grosenick et al., 2015; Lee et al., 2022). In the field of neuroscience, the closed-loop control system used for optogenetic modulation has been reported, where the input is a time-varying light stimulus and the output may be physiological parameters, such as electrophysiological, behavioral, pH, blood oxygen or glucose levels, or neurochemical changes associated with neurotransmitter release (Armstrong et al., 2013; Grosenick et al., 2015; Zaaimi et al., 2022). For example, Fig. 12.7F shows a wireless closed-loop optogenetic system inserted between the spinal cord and vertebrae to modulate muscle responses, which enables ultrafast, wireless, closed-loop manipulation of targeted neurons and pathways across the entire dorsoventral spinal cord in untethered mice (Kathe et al., 2022). This system is comprised of dual-color LEDs (red and blue), used for light activation and inhibition (input), and electrophysiological electrode, used for collecting electromyographic (EMG) signals. In vivo experiment results confirm that the system enables closed-loop control of optogenetic stimulation using real-time processing of physiological signals.

Conventional electronic devices can only be fabricated on a planar surface, which is mismatched with the shape of 3D biotissues, such as the heart, and brain. It is necessary to develop curvy electronics that can be assembled into devices on 3D surfaces without losing performance in some applications. Stretchable electronics create an

opportunity to meet this challenge. As shown in Fig. 12.7G, full 3D integration of electronics with the epicardial surface (Xu et al., 2014). Micro-LEDs and other several sensors are transferred onto 3D elastic membranes shaped precisely to match the epicardium of the heart. The electronic system completely envelops the heart, and possesses inherent elasticity, providing a mechanically stable biotic/abiotic interface during normal cardiac cycles. This integration scheme presents a promising opportunity to design and implement bioelectronics with complex structures.

12.3.2 Photodetectors

PDs are indispensable components for the light sensor, which are found in a variety of applications such as optical telecommunications, imaging, and biomedical sensing. In recent years, new flexible PD applications, such as e-eyes, oximeters, and flexible cameras, have attracted a great deal of research interest. Fig. 12.8A shows a wireless, injectable fluorescence photometer that integrates a LED and a PD on a flexible, needle-shaped polymer substrate (Lu, Gutruf, et al., 2018). The ultrathin geometry and compliant mechanics of these probes allow minimally invasive implantation. The fluorescence photometer can record neuronal activity using genes expressing calcium indicators, which is a standard fluorescent technique that detects Ca^{2+} changes associated with cell activity. In vivo studies in freely moving animals shows that the photometry can capture transient calcium fluorescence from active neurons in the deep brain (basolateral amygdala), demonstrating the capability to monitor neural activity in freely moving animals. The technology scheme that excitation light sources based on micro-LED, in collaboration with a PD for measuring transmission, reflection, and emission can also be used to fabricate the oximetry sensors. As shown in Fig. 12.8B, an epidermal optoelectronic device with the integration of red and infrared LEDs and a Si-based PD is fabricated for blood oxygen measurement based on Beer–Lambert law (Li et al., 2017). The reflected light is analyzed by a PD to determine the blood oxygen level in real-time. The epidermal optoelectronic device is attached to the wrist for demonstrating the practical application of the epidermal optoelectronic device. Similar photoelectric systems can also be used to monitor blood oxygen in biological tissues. Zhang et al. report a pair of micro-LEDs and a PD are integrated on a needle-shaped polymer substrate to form an implantable probe for measuring tissue oxygen saturation (Zhang, Gutruf, et al., 2019). The implantable oximeter enables monitoring regional tissue oxygen saturation levels in vivo, including deep brain regions, on freely moving animal models. Hong et al. report a low-cost, high-throughput flexible GaAs PD arrays fabrication scheme. GaAs PD arrays are grown on a Si substrate and transferred to a polyimide film via metal wafer bonding and epitaxial lift-off (Hong et al., 2020). 100% transfer yield of a 20×10 GaAs PD array is achieved. PD arrays that are highly uniform and thermal crack-free after the transfer process. The optical and

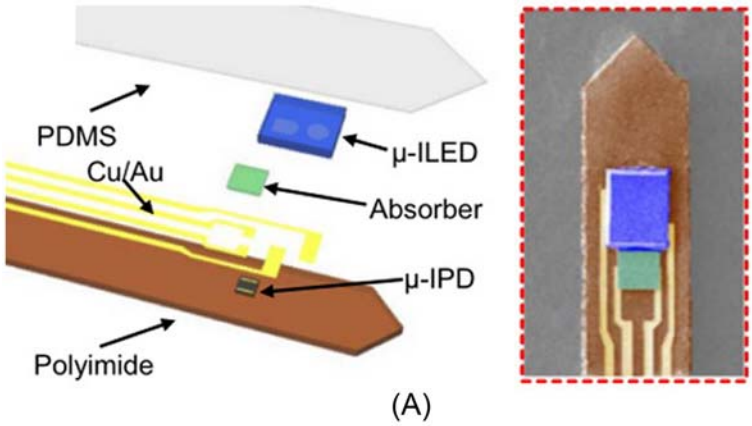

(A)

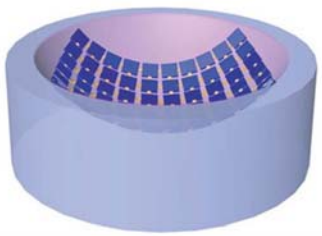

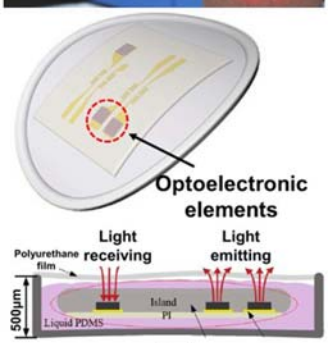

(B)

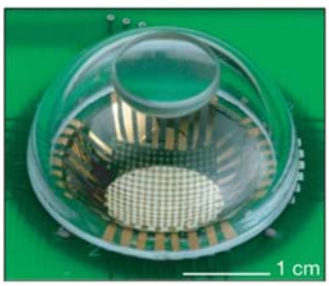

(C)

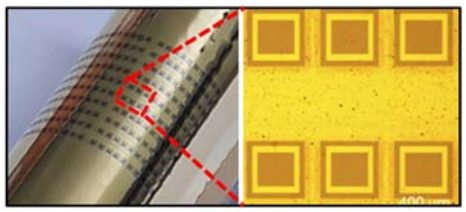

(D)

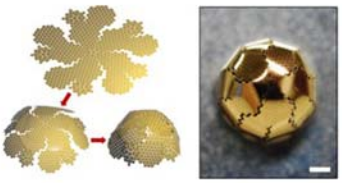

(E)

(*Continued*)

electrical properties of the GaAs PD array are almost the same before and after the transfer process. Fig. 12.8D shows a flexible GaAs PD array in a bent configuration. One thousand bending cycles of the flexible PD array confirm excellent durability. This technology offers an opportunity for large-scale optoelectronic device integration (Fig. 12.8).

The human eye is a remarkable imaging device, which has photoreceptors that capture and transduce photons into electrochemical signals. The eye-inspired optoelectronic systems have always attracted the attention of researchers due to their many unique features. Eyes enable a wide field of view and low aberrations with few-component imaging optics benefiting from a hemispherical detector geometry (Ko et al., 2008). Inspired by the eye, Ko et al. report a hemispherical electronic eye camera based on single-crystalline silicon PDs (shown in Fig. 12.8C) (Ko et al., 2008). The hemispherical PDMS substrate formed by casting PDMS in the gap between opposing convex and concave lenses with matching radii of curvature transform into the planar shape of a "drumhead" at sufficiently large radial tension. The focal plane PD array is fabricated on the silicon-on-insulator wafer and then peeled off from the wafer by etching the oxide layer and further transferred on the tensioned, planar drumhead shape PDMS substrate. Finally, the PDMS substrate with PD array returns to its initial hemispherical shape by releasing the radial tension. Fig. 12.8E illustrates a simple origami approach for fabricating Si-based focal plane arrays and artificial compound eyes that have hemisphere-like structures (Zhang, Jung, et al., 2017). The silicon-based devices are fabricated on the silicon-on-insulator wafer and shaped into maps of a truncated icosahedron, then transferred onto the PI substrate with a matching shape and further folded either into a concave or convex hemisphere. Those technologies provide practical routes for integrating planar devices onto complex curved surfaces.

Figure 12.8 Photodetectors (PD). (A) Implantable fluorescence photometer that combines light sources and PDs (*Left*: the schematic exploded-view illustration of photometry probe; *Right*: SEM image of the probe tip). (B) Wearable blood oxygen detection device that integrates LED and Si-based PD (*Upper*: the device integrated onto human wrist; *Bottom*: the illustration of blood oxygen detection device). (C) Eye-like optical imaging system based on compressible silicon optoelectronics (the schematic illustrating (*upper*) and optical image (*bottom*) of eye-like optical imaging system). (D) Flexible GaAs PD arrays for wearable photonics platform (Left: the image of the flexible PD mounted on a curved surface; Right: the optical microscope image of PD array). (E) The hemispherical electronic eye systems based on origami silicon nanomembrane-based photodiode (*Left*: the schematic illustration of the net of half truncated icosahedron being folded into a hemisphere; *Right*: a photograph of the half truncated icosahedron). *(A) Reproduced with permission from. Copyright © 2018. Published under the PNAS license; (B) Reproduced with permission from. Copyright © 2017 WILEY-VCH Verlag GmbH & Co. KGaA, Weinheim; (C) Reproduced with permission from. Copyright © 2008, Macmillan Publishers Limited; (D) Reproduced with permission from. Copyright © 2020 Optical Society of America; (E) Reproduced with permission from. Copyright © 2017, The Author (s).*

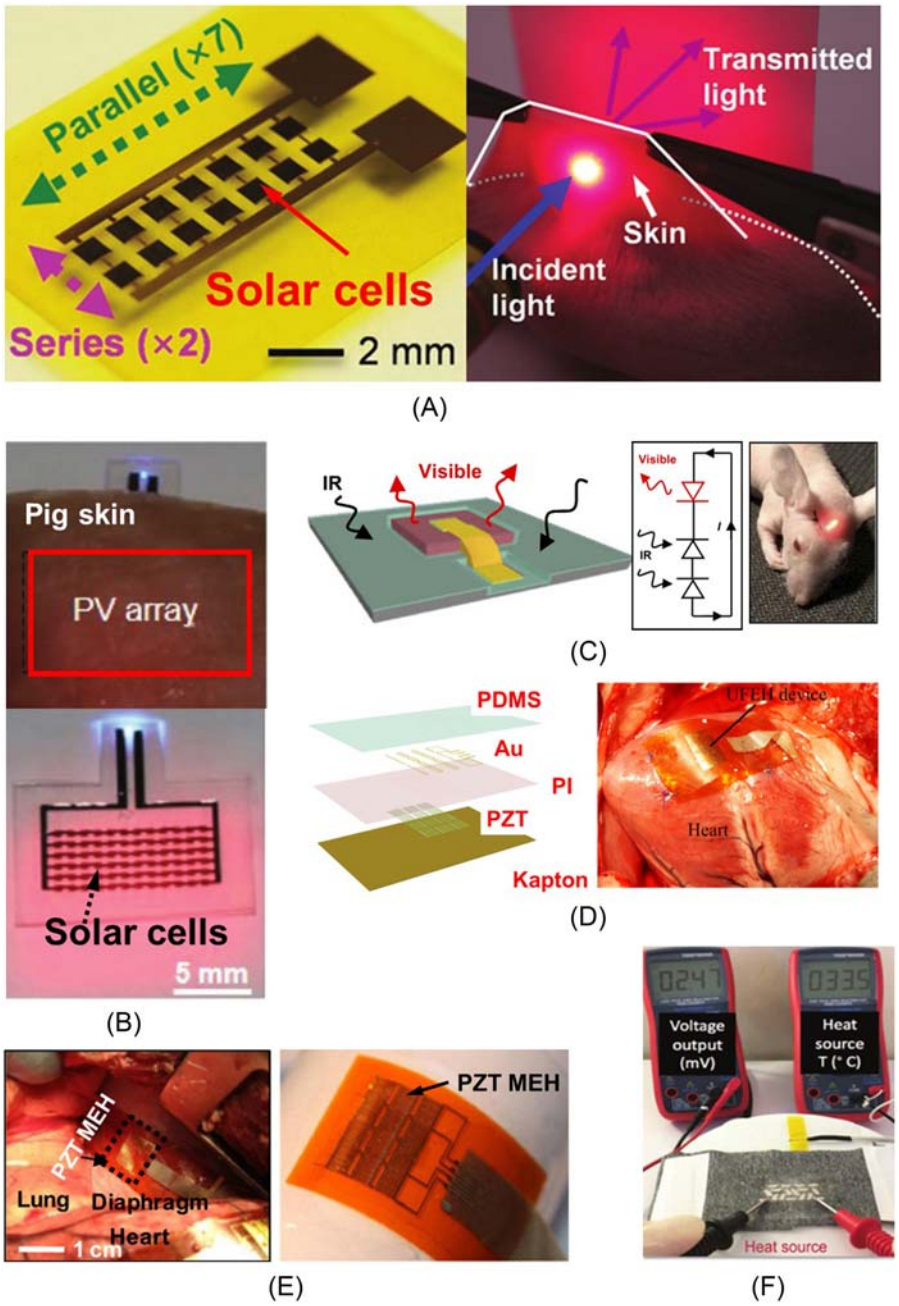

Figure 12.9 Energy-harvesting devices. (A) Implantable solar cell arrays for powering medical electronics (*Left*: the optical image of solar cell arrays; *Right*: the schematic illustration of a potential

(*Continued*)

12.3.3 Energy-harvesting devices

Despite significant advances in the area, the power supply is a critical challenge for flexible bioelectronic devices, which require stable operation without behavioral or environmental restrictions. Conventional devices usually use external batteries to provide sufficient and stable power, whose electrical capacities, size, and weight is barriers to further minimization. Various innovative approaches are being proposed for power in bioelectronic devices, using mechanical movement, photovoltaic (PV) conversion, thermoelectric effect, and others. Flexible solar cells have been actively developed as attractive power sources for bioelectronic devices. Song et al. report a flexible solar cell array for powering medical electronics. The schematic illustration of a solar cell is shown in Fig. 12.9A left photo (Song et al., 2016). The dual junction (GaInP: bandgap ≈ 1.8 eV, GaAs: bandgap ≈ 1.4 eV) solar microcells are fabricated and released from the original wafer with an elastomeric stamp (PDMS) and further transferred onto a PI film. To demonstrate the in vivo electrical performances, a solar cell array is implanted into live mouse models. The subdermally solar cell array generates approximately 647 μW of direct current power, which can power a custom-built flexible pacemaker. Based on bioresorbable materials, including Si, Mo, and PLGA. As shown in Fig. 12.9B, Lu et al. develop a fully biodegradable, monocrystalline silicon PV platform (Lu, Yang, et al., 2018). Si-solar cells are fabricated on SOI substrate with Mo interconnections and poly (lactic-*co*-glycolic acid) (PLGA) as an encapsulation layer and released from the silicon wafer by backside etching. The remaining buried oxide layer underneath the microcells serves as a back biofluid barrier for the array. The Si-solar cell array (including 72 solar cells) can generate ≈ 60 μW of electrical power under 4 mm of porcine skin. The solar

application of solar cell arrays that power implantable electronics). (B) Monocrystalline silicon photovoltaic microcells as power supplies for biomedical implants (*Upper*: Si PV array under pig skin and fat; *Bottom*: Si PV array after immersion in PBS solution). (C) The infrared-to-visible upconversion devices as injectable light sources (*Left*: The schematic illustration of the fabricated upconversion device; Middle: the operational principle of the upconversion device design; *Right*: the image of a mouse with devices implanted). (D) The ultra-flexible energy harvester (UFEH) based on piezoelectric devices for harvesting the biomechanical energy (*Left*: the schematic illustration of UFEH; *Right*: the image of UFEH mounted between left ventricular apex and right ventricle). (E) The piezoelectric energy harvester integrated with heart, lung, and diaphragm. (F) The thermoelectric generator for body heat harvesting (*Left*: the photograph of a PZT energy harvester on the bovine diaphragm; *Right*: the photograph of the PZT energy harverster). *(A) Reproduced with permission from. Copyright © 2016 WILEY-VCH Verlag GmbH & Co. KGaA, Weinheim; (B) Reproduced with permission from. Copyright © 2018 WILEY-VCH Verlag GmbH & Co. KGaA, Weinheim; (C) Reproduced with permission from. Copyright © 2018. Published under the PNAS license; (D) Reproduced with permission from. Copyright © 2015, The Author (s); (E) Reproduced with permission from. Copyright © 2014. Published under the PNAS license; (F) Reproduced with permission from. Copyright © 2019 WILEY-VCH Verlag GmbH & Co. KGaA, Weinheim.*

cell array fully dissolves in biofluids after 4 months, and the degradation process introduces no inflammatory responses in the surrounding tissues. These characteristics illustrate the potential for using silicon solar cells as bioresorbable power supplies for various transient biomedical implants (Fig. 12.9).

As shown in Fig. 12.9C, an infrared-to-visible upconversion microscale device is achieved based on the full integration of solar cells and LED (Ding et al., 2018). The upconversion device includes a includes connected double junction gallium arsenide (GaAs) solar cell and an aluminum gallium indium phosphide (AlGaInP)-based visible LED. GaAs-based solar cell captures low-energy near-infrared photons, providing photogenerated currents and voltages that drive the visible LED. The device is fabricated on GaAs substrates and released by etching sacrificial layer and further can be integrated with various heterogeneous substrates via transfer printing. The encapsulated microscale device can be implanted in the subcutaneous tissue and provides stable, long-term implantable light sources in behavioral animals. This approach provides a feasible route for developing passive wireless implantable light sources.

Mechanical energy is an important source of energy for powering bioelectronics. The human body produces abundant kinetic energy, such as the motion of the heart, and the contraction/relaxation of the diaphragm and lungs. For instance, the cardiac output power is about 1.4 W, which is enough to power many bioelectronic devices. Piezoelectric materials are capable of mechanical-to-electrical energy conversion, which offer practical routes to energy harvesting in vivo. As a common piezoelectric material, lead zirconate titanate (PZT) has already been used to collect biomechanical energy from the motion of the heart, lung, and diaphragm. Dagdeviren et al. report a flexible PZT mechanical energy harvester (Fig. 12.9E) (Dagdeviren et al., 2014). The key functional elements of the energy harvester consist of 12 groups of 10 PZT ribbons transferred onto the PI substrate. In vivo studies demonstrated that PZT energy harvesters enable high-efficiency mechanical-to-electrical energy conversion from the natural contractile and relaxation motions of the heart, lung, and diaphragm. The devices exhibit excellent mechanical and electrical stability. There is no noticeable degradation in the properties after over 20 million bending/releasing cycles in moist environments. Fig. 12.9D shows an ultra-flexible PZT energy harvester used to harvest biomechanical energy from heart motions (Lu et al., 2015). The brittle piezoelectric film with high piezoelectric coefficients is integrated onto the extremely soft PI substrate via transfer printing technology. The PZT energy harvester is implanted in pigs under different conditions, such as with an open or closed chest, or awake or under anesthesia. The output voltage can be up to 3 V, which is approximately the same as the required value for biomedical implants.

Body heat can be an inexhaustible source of energy during the lifespan of a person because the core body temperature is regulated at 37°C. The total heat dissipated from the whole human body is approximately 60−180 W depending on body activity (Riemer & Shapiro, 2011), which is a very attractive energy source.

Thus, thermoelectric generators have attracted the attention of academic researchers. Elmoughni et al. report a textile-integrated thermoelectric generator for body heat harvesting to power wearable electronics (Elmoughni et al., 2019). A 32-leg device with a modest fill factor ($\approx 30\%$) is fabricated on a commercial sports fabric substrate via stencil and transfer printing techniques (shown in Fig. 12.9F). The textile-integrated thermoelectric generator yields an open circuit voltage of ≈ 3 mV at $\Delta T = 3$ K (Elmoughni et al., 2019). The fabrication technology offers new opportunities for advancing thermoelectric material integration into clothing.

12.3.4 Bioresorbable materials and devices

Biodegradable electronics that can partially or completely decompose, dissolve, degrade, resorb or physically disappear into physiological or environmental solutions in a well-regulated way, after the desired lifetime, thereby eliminating the costs, complications, and risks associated with secondary surgical procedures for device retrieval (Choi et al., 2020; Li et al., 2018; Rajaram et al., 2022; Singh et al., 2000). This chapter focus on inorganic bioresorbable electronic systems in biomedicine fabricated by transferring printing technology. Compared to organic materials, inorganics offer excellent electrical performance. Inorganic biodegradable materials include monocrystalline silicon (mono-Si), polycrystalline silicon (poly-Si), amorphous silicon (a-Si), germanium (Ge), silicon germanium alloy (SiGe), indium−gallium−zinc oxide (a-IGZO), and zinc oxide (ZnO) for semiconductors; magnesium (Mg), molybdenum (Mo), tungsten (W), iron (Fe), and zinc (Zn) for conductive materials; and magnesium oxide (MgO), silicon dioxide (SiO_2), and silicon nitride (SiN_x) for dielectric materials (Li et al., 2018). Biodegradable electronics have been made for a variety of biomedical applications, such as biomedical sensors, stimulators, and photonic devices. Fig. 12.10A shows the representative flexible biodegradable circuit based on dissolvable inorganic silicon-based CMOS, including transistors made by Si/MgO/Mg, diodes made by Si, and inductors and capacitors made by Mg/MgO, as well as resistor and connection wires made by Mg. Si-based COMS is the key component of the electronics, which is fabricated on an SOI wafer and transferred onto a silk substrate (Hwang et al., 2012). All of the components, including inductors, capacitors, resistors, diodes, transistors, interconnects, substrates, and encapsulation layers, disintegrate and dissolve over controlled periods when immersed in deionized (DI) water (Fig. 12.10).

Various transient sensors fabricated by inorganic biodegradable materials are proposed. As shown in Fig. 12.10B (Hwang et al., 2015), The transient stretchable pH sensors are built using doped Si nanoribbons via transfer printing technology. Mg serves as the electrodes and interconnects, and SiO_2 serves as the interlayer dielectrics and encapsulants. Studies show that dissolve kinetics depend strongly on temperature, pH, and ionic content/concentration of solutions, as well as the morphologies of the materials. Kang et al. report a biodegradable pressure sensor based on the piezoresistive

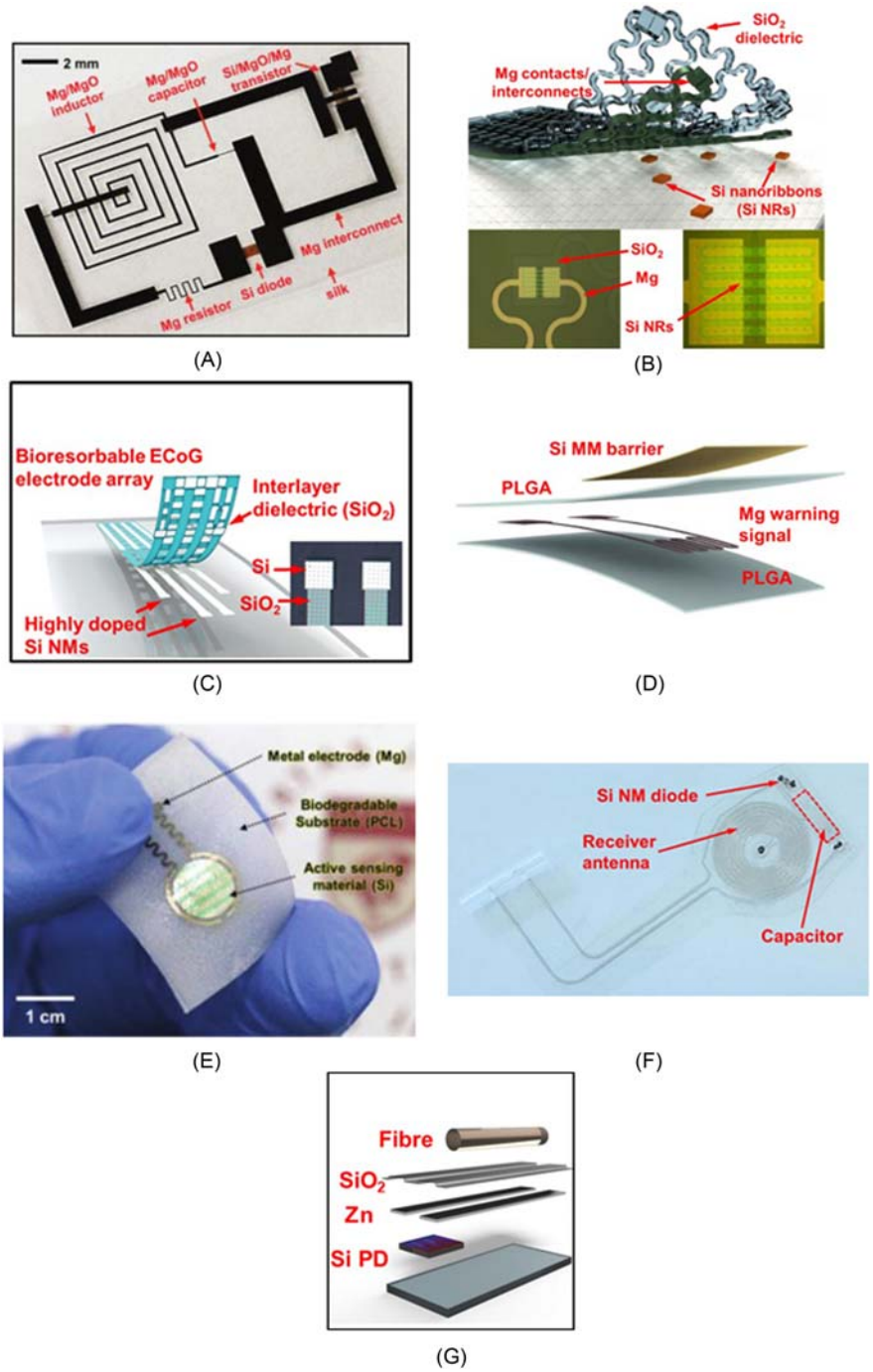

Figure 12.10 Bioresorbable materials and devices. (A) The transient electronics platform: includes transistors, diodes, capacitors, and resistors. (B) The transient electronics and biosensors based on

(*Continued*)

Si nanomembrane (Kang et al., 2016). Si nanomembrane is formed on SOI wafer and then transferred onto poly (lactic-*co*-glycolic acid) (PLGA) substrate. The resistance of this sensing element increases monotonically in a linear fashion across the full range of pressures that are relevant to intracranial monitoring (that is, 0−70 mmHg). Monocrystalline silicon nanomembrane array can also be used to fabricate ECoG electrodes, as shown in Fig. 12.10C (Yu et al., 2016). In vivo studies confirm the capability for recording electrophysiological signals from the cortical surface and the subgaleal space. The devices detect normal physiologic and epileptiform activity, both in acute and chronic recordings. Yang et al. report a sensor for the onset of water penetration. The failure of implanted electronic devices mostly starts from water penetration. Evaluating water penetration can be extremely useful in cases where the encapsulation unexpectedly fails for implantable electronics. A schematic illustration of water penetration is shown in Fig. 12.10D (Yang et al., 2020). the addition of an Mg resistor at the middle position of the PLGA layer underneath the Si micromembranes (MMs) can serve as a sensor for water penetration. Si MM is fabricated on SOI substrate and transferred onto PLGA as an encapsulation layer. The studies show that the sudden increase in Mg resistance can reflect water penetration. A transient electrochemical sensor is shown in Fig. 12.10E (Kim et al., 2018). Ultrathin monocrystalline silicon nanomembranes coated with iron (Fe)-containing nanoparticles (NPs) as a catalyst serve as active sensing elements for continuous, real-time monitoring of dopamine secretion, which is integrated with biodegradable polycaprolactone substrate via transfer printing. All of the materials are gradually hydrolyzed or dissolved in the PBS (pH 11, 37°C) via reactive diffusion, and most of the components disappear in $\approx$15 hours. Dissolution rates can be adjusted by pH, temperature, and ionic contents and concentrations of solutions.

biodegradable silicon nanomembranes; *Upper*: the exploded view schematic illustration of the device; *Bottom*: the optical microscope image of an individual pH sensor (*left*) and its magnified view. (C) The bioresorbable neural electrode array for ECoG and subdermal EEG measurements based on silicon electronics. (D) The bioresorbable sensor for the onset of water penetration in the intracranial space. (E) The transient electrochemical sensor based on silicon nanomembranes. (F) The bioresorbable electronic neuro regenerative medical device. (G) The transient photonic platform for the continuous monitoring of cerebral temperature, oxygenation and neural activity in freely moving mice. *(A) Reproduced with permission from. Copyright © 2012, American Association for the Advancement of Science; (B) Reproduced with permission from. Copyright © 2015 American Chemical Society; (C) Reproduced with permission from. Copyright © 2016, Nature Publishing Group; (D) Reproduced with permission from. Copyright © 2020 WILEY-VCH Verlag GmbH & Co. KGaA, Weinheim; (E) Reproduced with permission from. Copyright © 2018 WILEY-VCH Verlag GmbH & Co. KGaA, Weinheim; (F) Reproduced with permission from. Copyright © 2018, The Author (s), under exclusive licence to Springer Nature America, Inc; (G) Reproduced with permission from. Copyright © 2019, The Author (s), under exclusive licence to Springer Nature Limited.*

Koo et al. report a bioresorbable, wireless electrical stimulator used as an electronic neuro-regenerative medical device (shown in Fig. 12.10F) (Koo et al., 2018). The stimulator includes a loop antenna made of Mg, a RF diode made of silicon nanomembrane with electrodes of Mg, a parallel plate capacitor made of Mg/SiO_2/Mg, and a stimulation electrode made of Mg or Mo strip. In vivo experiments demonstrate that electrical stimulation enables enhances and accelerates neuron functional recovery.

Implantable biodegradable photonic devices are composed for the spectroscopic characterization of targeted tissues and biofluids. As shown in Fig. 12.10G (Bai et al., 2019), the devices incorporate a collection of bioresorbable optical components which are heterogeneously integrated into PLGA fiber via the transfer printing method, including single-junction PDs based on Si nanomembranes; foundry-produced tri-color PDs based on tri-layer stacks of Si P−N junctions; optical multilayer filters of SiO_x and SiN_y. The devices are implanted into deep brain regions of freely moving mice for continuous absorption spectroscopic analysis of biochemical and physiological status.

12.4 Conclusion

This chapter provides an overview of heterogeneously integrated inorganic materials and devices for biomedical applications. Diverse and disparate classes of materials and functional devices, including metals, oxides, semiconductors, 2D materials, biomaterials, optoelectronics, energy-harvesting devices, and bioresorbable materials and devices, can be assembled into single and multifunctional systems. Such materials and functional devices can serve a variety of roles in bioelectronic devices, such as electrodes, antennae, heat sinkers, sensors, stimulators, and energy harvesters. Transfer printing is a highly versatile technique for the heterogeneous integration of bioelectronic devices with other components and circuits in 2D and 3D layouts. This technology enables the cointegration of a broad spectrum of materials regardless of conditions for their growth, deposition, or patterning, and thereby maximizes their performance and cost-effectiveness or imparts novel hybrid functionalities. More and more multifunctional bioelectronic devices will be developed via transfer printing technology. These multifunctional bioelectronic devices can provide unprecedented advantages in healthcare applications.

References

Armstrong, C., Krook-Magnuson, E., Oijala, M., & Soltesz, I. (2013). Closed-loop optogenetic intervention in mice. *Nature Protocols*, *8*(8), 1475−1493. Available from https://doi.org/10.1038/nprot.2013.080.

Bai, W., Shin, J., Fu, R., Kandela, I., Lu, D., Ni, X., Park, Y., Liu, Z., Hang, T., Wu, D., Liu, Y., Haney, C. R., Stepien, I., Yang, Q., Zhao, J., Nandoliya, K. R., Zhang, H., Sheng, X., Yin, L., … Rogers, J. A. (2019). Bioresorbable photonic devices for the spectroscopic characterization of physiological status and neural activity. *Nature Biomedical Engineering*, *3*(8), 644−654. Available from https://doi.org/10.1038/s41551-019-0435-y, http://www.nature.com/natbiomedeng/.

Behl, M., & Lendlein, A. (2007). Shape-memory polymers. *Materials Today*, *10*(4), 20–28. Available from https://doi.org/10.1016/S1369-7021(07)70047-0.

Bendali, A., Rousseau, L., Lissorgues, G., Scorsone, E., Djilas, M., Dégardin, J., Dubus, E., Fouquet, S., Benosman, R., Bergonzo, P., Sahel, J. A., & Picaud, S. (2015). Synthetic 3D diamond-based electrodes for flexible retinal neuroprostheses: Model, production and in vivo biocompatibility. *Biomaterials*, *67*, 73–83. Available from https://doi.org/10.1016/j.biomaterials.2015.07.018, http://www.journals.elsevier.com/biomaterials/.

Cao, Y., Wang, S., Lv, J., Li, F., Liang, Q., Yang, M., Ma, X., Wang, H., & Hao, Y. (2022). Fully physically transient volatile memristor based on Mg/magnesium oxide for biodegradable neuromorphic electronics. *IEEE Transactions on Electron Devices*, *69*(6), 3118–3123. Available from https://doi.org/10.1109/TED.2022.3166868, https://ieeexplore.ieee.org/xpl/mostRecentIssue.jsp?punumber = 16.

Carlson, A., Bowen, A. M., Huang, Y., Nuzzo, R. G., & Rogers, J. A. (2012). Transfer printing techniques for materials assembly and micro/nanodevice fabrication. *Advanced Materials*, *24*(39), 5284–5318. Available from https://doi.org/10.1002/adma.201201386.

Chen, Y., Zhang, Y., Liang, Z., Cao, Y., Han, Z., & Feng, X. (2020). Flexible inorganic bioelectronics. *Npj Flexible Electronics*.

Choi, Y., Koo, J., & Rogers, J. A. (2020). Inorganic materials for transient electronics in biomedical applications. *MRS Bulletin*, *45*(2), 103–112. Available from https://doi.org/10.1557/mrs.2020.25, http://journals.cambridge.org/MRS.

Choi, C., Lee, Y., Cho, K. W., Koo, J. H., & Kim, D. H. (2019). Wearable and implantable soft bioelectronics using two-dimensional materials. *Accounts of Chemical Research*, *52*(1), 73–81. Available from https://doi.org/10.1021/acs.accounts.8b00491, https://doi.org/10.1021/acs.accounts.8b00491.

Corbett, B., Loi, R., Zhou, W., Liu, D., & Ma, Z. (2017). Transfer print techniques for heterogeneous integration of photonic components. *Progress in Quantum Electronics*, *52*, 1–17. Available from https://doi.org/10.1016/j.pquantelec.2017.01.001.

Coyer, S. R., García, A. J., & Delamarche, E. (2007). Facile preparation of complex protein architectures with sub-100-nm resolution on surfaces. *Angewandte Chemie - International Edition*, *46*(36), 6837–6840. Available from https://doi.org/10.1002/anie.200700989.

Dagdeviren, C., Yang, B. D., Su, Y., Tran, P. L., Joe, P., Anderson, E., Xia, J., Doraiswamy, V., Dehdashti, B., Feng, X., Lu, B., Poston, R., Khalpey, Z., Ghaffari, R., Huang, Y., Slepian, M. J., & Rogers, J. A. (2014). Conformal piezoelectric energy harvesting and storage from motions of the heart, lung, and diaphragm. *Proceedings of the National Academy of Sciences*, *111*(5), 1927–1932. Available from https://doi.org/10.1073/pnas.1317233111.

Ding, H., Lu, L., Shi, Z., Wang, D., Li, L., Li, X., Ren, Y., Liu, C., Cheng, D., Kim, H., Giebink, N. C., Wang, X., Yin, L., Zhao, L., Luo, M., & Sheng, X. (2018). Microscale optoelectronic infrared-to-visible upconversion devices and their use as injectable light sources. *Proceedings of the National Academy of Sciences*, *115*(26), 6632–6637. Available from https://doi.org/10.1073/pnas.1802064115.

Elmoughni, H. M., Menon, A. K., Wolfe, R. M., & Yee, S. K. (2019). A textile-integrated polymer thermoelectric generator for body heat harvesting. *Advanced Materials Technologies*, *2019*(7).

Fallegger, F., Schiavone, G., & Lacour, S. P. (1903). Conformable hybrid systems for implantable bioelectronic interfaces. *Advanced Materials*, *2020*(15).

Fang, H., Zhao, J., Yu, K. J., Song, E., Farimani, A. B., Chiang, C. H., Jin, X., Xue, Y., Xu, D., Du, W., Seo, K. J., Zhong, Y., Yang, Z., Won, S. M., Fang, G., Choi, S. W., Chaudhuri, S., Huang, Y., Alam, M. A., … Rogers, J. A. (2016). Ultrathin, transferred layers of thermally grown silicon dioxide as biofluid barriers for biointegrated flexible electronic systems. *Proceedings of the National Academy of Sciences of the United States of America*, *113*(42), 11682–11687. Available from https://doi.org/10.1073/pnas.1605269113, http://www.pnas.org/content/113/42/11682.full.pdf.

Fan, B., Rusinek, C. A., Thompson, C. H., Setien, M., Guo, Y., Rechenberg, R., Gong, Y., Weber, A. J., Becker, M. F., & Purcell, E. (2020). Flexible, diamond-based microelectrodes fabricated using the diamond growth side for neural sensing. *Microsystems & Nanoengineering*, *2020*(1), 1–12.

Feron, K., Lim, R., Sherwood, C., Keynes, A., Brichta, A., & Dastoor, P. C. (2018). Organic bioelectronics: Materials and biocompatibility. *International Journal of Molecular Sciences*, *19*(8). Available from https://doi.org/10.3390/ijms19082382, http://www.mdpi.com/journal/ijms.

Grosenick, L., Marshel, J. H., & Deisseroth, K. (2015). Closed-loop and activity-guided optogenetic control. *Neuron*, *86*(1), 106–139. Available from https://doi.org/10.1016/j.neuron.2015.03.034, http://www.cell.com/neuron/home.

Gutruf, P., & Rogers, J. A. (2018). Implantable, wireless device platforms for neuroscience research. *Current Opinion in Neurobiology*, *50*, 42–49. Available from https://doi.org/10.1016/j.conb.2017.12.007, http://www.elsevier.com/locate/conb.

Hess, A. E., Sabens, D. M., Martin, H. B., & Zorman, C. A. (2011). Diamond-on-polymer microelectrode arrays fabricated using a chemical release transfer process. *Journal of Microelectromechanical Systems*, *20*(4), 867–875. Available from https://doi.org/10.1109/JMEMS.2011.2159099.

He, P., Peng, Y., & Lin, L. (2021). A multimodal self-healing flexible sweat sensor for healthcare monitoring. In *Proceedings of the IEEE international conference on micro electro mechanical systems (MEMS)*. Institute of Electrical and Electronics Engineers Inc., United States, pp. 517–520. 9781665419123. 10.1109/MEMS51782.2021.9375234.

Hong, N., Chu, R. J., Kang, S. S., Ryu, G., Han, J.-H., Yu, K. J., Jung, D., & Choi, W. J. (2020). Flexible GaAs photodetector arrays hetero-epitaxially grown on GaP/Si for a low-cost III-V wearable photonics platform. *Optics Express*, *2020*(24), 36559–36567.

Hwang, S. W., Lee, C. H., Cheng, H., Jeong, J. W., Kang, S. K., Kim, J. H., Shin, J., Yang, J., Liu, Z., Ameer, G. A., Huang, Y., & Rogers, J. A. (2015). Biodegradable elastomers and silicon nanomembranes/nanoribbons for stretchable, transient electronics, and biosensors. *Nano Letters*, *15*(5), 2801–2808. Available from https://doi.org/10.1021/nl503997m, http://pubs.acs.org/journal/nalefd.

Hwang, S. W., Tao, H., Kim, D. H., Cheng, H., Song, J. K., Rill, E., Brenckle, M. A., Panilaitis, B., Won, S. M., Kim, Y. S., Song, Y. M., Yu, K. J., Ameen, A. A., Li, R., Su, Y., Yang, M., Kaplan, D. L., Zakin, M. R., Slepian, M. J., … Rogers, J. A. (2012). A physically transient form of silicon electronics. *Science (New York, N.Y.)*, *337*(6102), 1640–1644. Available from https://doi.org/10.1126/science.1226325, http://www.sciencemag.org/content/337/6102/1640.full.pdf.

Jeong, J. W., McCall, J. G., Shin, G., Zhang, Y., Al-Hasani, R., Kim, M., Li, S., Sim, J. Y., Jang, K. I., Shi, Y., Hong, D. Y., Liu, Y., Schmitz, G. P., Xia, L., He, Z., Gamble, P., Ray, W. Z., Huang, Y., Bruchas, M. R., & Rogers, J. A. (2015). Wireless optofluidic systems for programmable in vivo pharmacology and optogenetics. *Cell*, *162*(3), 662–674. Available from https://doi.org/10.1016/j.cell.2015.06.058, https://www.sciencedirect.com/journal/cell.

Jin, S. H., Kang, S. K., Cho, I. T., Han, S. Y., Chung, H. U., Lee, D. J., Shin, J., Baek, G. W., Kim, T. I., Lee, J. H., & Rogers, J. A. (2015). Water-soluble thin film transistors and circuits based on amorphous indium-gallium-zinc oxide. *ACS Applied Materials and Interfaces*, 7(15), 8268–8274. Available from https://doi.org/10.1021/acsami.5b00086, http://pubs.acs.org/journal/aamick.

Kang, S. K., Murphy, R. K. J., Hwang, S. W., Lee, S. M., Harburg, D. V., Krueger, N. A., Shin, J., Gamble, P., Cheng, H., Yu, S., Liu, Z., McCall, J. G., Stephen, M., Ying, H., Kim, J., Park, G., Webb, R. C., Lee, C. H., Chung, S., … Rogers, J. A. (2016). Bioresorbable silicon electronic sensors for the brain. *Nature*, *530*(7588), 71–76. Available from https://doi.org/10.1038/nature16492, http://www.nature.com/nature/index.html.

Kathe, C., Michoud, F., Schönle, P., Rowald, A., Brun, N., Ravier, J., Furfaro, I., Paggi, V., Kim, K., Soloukey, S., Asboth, L., Hutson, T. H., Jelescu, I., Philippides, A., Alwahab, N., Gandar, J., Huber, D., De Zeeuw, C. I., Barraud, Q., … Courtine, G. (2022). Wireless closed-loop optogenetics across the entire dorsoventral spinal cord in mice. *Nature Biotechnology*, *40*(2), 198–208. Available from https://doi.org/10.1038/s41587-021-01019-x, http://www.nature.com/nbt/index.html.

Khang, D. Y., Jiang, H., Huang, Y., & Rogers, J. A. (2006). A stretchable form of single-crystal silicon for high-performance electronics on rubber subtrates. *Science (New York, N.Y.)*, *311*(5758), 208–212. Available from https://doi.org/10.1126/science.1121401.

Kim, Y. S., Basir, A., Herbert, R., Kim, J., Yoo, H., & Yeo, W. H. (2020). Soft materials, stretchable mechanics, and optimized designs for body-wearable compliant antennas. *ACS Applied Materials and Interfaces*, *12*(2), 3059–3067. Available from https://doi.org/10.1021/acsami.9b20233, http://pubs.acs.org/journal/aamick.

Kim, D. H., Lu, N., Ma, R., Kim, Y. S., Kim, R. H., Wang, S., Wu, J., Won, S. M., Tao, H., Islam, A., Yu, K. J., Kim, T. I., Chowdhury, R., Ying, M., Xu, L., Li, M., Chung, H. J., Keum, H.,

McCormick, M., ... Rogers, J. A. (2011). Epidermal electronics. *Science (New York, N.Y.)*, *333* (6044), 838–843. Available from https://doi.org/10.1126/science.1206157, http://www.sciencemag.org/content/333/6044/838.full.pdf, United States.

Kim, T. I., McCall, J. G., Jung, Y. H., Huang, X., Siuda, E. R., Li, Y., Song, J., Song, Y. M., Pao, H. A., Kim, R. H., Lu, C., Lee, S. D., Song, I. S., Shin, G., Al-Hasani, R., Kim, S., Tan, M. P., Huang, Y., Omenetto, F. G., ... Bruchas, M. R. (2013). Injectable, cellular-scale optoelectronics with applications for wireless optogenetics. *Science (New York, N.Y.)*, *340*(6129), 211–216. Available from https://doi.org/10.1126/science.1232437, http://www.sciencemag.org/content/340/6129/211.full.pdf.

Kim, Y., Suh, J. M., Shin, J., Liu, Y., Yeon, H., Qiao, K., Kum, H. S., Kim, C., Lee, H. E., Choi, C., Kim, H., Lee, D., Lee, J., Kang, J. H., Park, B. I., Kang, S., Kim, J., Kim, S., Perozek, J. A., ... Kim, J. (2022). Chip-less wireless electronic skins by remote epitaxial freestanding compound semiconductors. *Science (New York, N.Y.)*, *377*(6608), 859–864. Available from https://doi.org/10.1126/science.abn7325, https://www.science.org/doi/10.1126/science.abn7325.

Kim, H. S., Yang, S. M., Jang, T. M., Oh, N., Kim, H. S., & Hwang, S. W. (2018). Bioresorbable silicon nanomembranes and iron catalyst nanoparticles for flexible, transient electrochemical dopamine monitors. *Advanced Healthcare Materials*, *7*(24). Available from https://doi.org/10.1002/adhm.201801071, https://onlinelibrary.wiley.com/journal/10.1002/(ISSN)2192-2659.

Koo, J., MacEwan, M. R., Kang, S. K., Won, S. M., Stephen, M., Gamble, P., Xie, Z., Yan, Y., Chen, Y. Y., Shin, J., Birenbaum, N., Chung, S., Kim, S. B., Khalifeh, J., Harburg, D. V., Bean, K., Paskett, M., Kim, J., Zohny, Z. S., ... Rogers, J. A. (2018). Wireless bioresorbable electronic system enables sustained nonpharmacological neuroregenerative therapy. *Nature Medicine*, *24*(12), 1830–1836. Available from https://doi.org/10.1038/s41591-018-0196-2, http://www.nature.com/nm/index.html.

Ko, H. C., Stoykovich, M. P., Song, J., Malyarchuk, V., Choi, W. M., Yu, C. J., Geddes, J. B., Xiao, J., Wang, S., Huang, Y., & Rogers, J. A. (2008). A hemispherical electronic eye camera based on compressible silicon optoelectronics. *Nature*, *454*(7205), 748–753. Available from https://doi.org/10.1038/nature07113, http://www.nature.com/nature/index.html.

Kuzum, D., Takano, H., Shim, E., Reed, J. C., Juul, H., Richardson, A. G., De Vries, J., Bink, H., Dichter, M. A., Lucas, T. H., Coulter, D. A., Cubukcu, E., & Litt, B. (2014). Transparent and flexible low noise graphene electrodes for simultaneous electrophysiology and neuroimaging. *Nature Communications*, *5*. Available from https://doi.org/10.1038/ncomms6259, http://www.nature.com/ncomms/index.html.

Lee, H., Choi, T. K., Lee, Y. B., Cho, H. R., Ghaffari, R., Wang, L., Choi, H. J., Chung, T. D., Lu, N., Hyeon, T., Choi, S. H., & Kim, D. H. (2016). A graphene-based electrochemical device with thermoresponsive microneedles for diabetes monitoring and therapy. *Nature Nanotechnology*, *11*(6), 566–572. Available from https://doi.org/10.1038/nnano.2016.38, http://www.nature.com/nnano/index.html.

Lee, K. J., Koo., & Park. (2012). Biointegrated flexible inorganic light emitting diodes. *Nanobiosensors in Disease Diagnosis*, *5*. Available from https://doi.org/10.2147/NDD.S26593.

Lee, H., Lee, J., Kim, S., & Lee, D. (2022). Implantable micro-light-emitting diode (μLED)-based optogenetic interfaces toward human applications. *Advanced Drug Delivery Reviews*, *187*.

Lee, W. S., Sunkara, V., Han, J. R., Park, Y. S., & Cho, Y. K. (2015). Electrospun TiO_2 nanofiber integrated lab-on-a-disc for ultrasensitive protein detection from whole blood. *Lab on a Chip*, *15*(2), 478–485. Available from https://doi.org/10.1039/c4lc00900b, http://pubs.rsc.org/en/journals/journal/lc.

Liao, F., Zhu, Z., Yan, Z., Yao, G., Huang, Z., Gao, M., Pan, T., Zhang, Y., Li, Q., & Feng, X. (2017). Ultrafast response flexible breath sensor based on vanadium dioxide. *Journal of Breath Research*, *2017*(3).

Lim, S., Son, D., Kim, J., Lee, Y. B., Song, J. K., Choi, S., Lee, D. J., Kim, J. H., Lee, M., Hyeon, T., & Kim, D. H. (2015). Transparent and stretchable interactive human machine interface based on patterned graphene heterostructures. *Advanced Functional Materials*, *25*(3), 375–383. Available from https://doi.org/10.1002/adfm.201402987, http://onlinelibrary.wiley.com/journal/10.1002/(ISSN)1616-3028.

Lin, J., Peng, Z., Liu, Y., Ruiz-Zepeda, F., Ye, R., Samuel, E. L. G., Yacaman, M. J., Yakobson, B. I., & Tour, J. M. (2014). Laser-induced porous graphene films from commercial polymers. *Nature Communications*, *5*. Available from https://doi.org/10.1038/ncomms6714, http://www.nature.com/ncomms/index.html.

Li, K., Chang, T. H., Li, Z., Yang, H., Fu, F., Li, T., Ho, J. S., & Chen, P. Y. (2019). Biomimetic MXene textures with enhanced light-to-heat conversion for solar steam generation and wearable thermal management. *Advanced Energy Materials*, *2019*(34), 1901.

Li, L., Lu, L., Ren, Y., Tang, G., Zhao, Y., Cai, X., Shi, Z., Ding, H., Liu, C., & Cheng, D. (2022). Colocalized, bidirectional optogenetic modulations in freely behaving mice with a wireless dual-color optoelectronic probe. *Nature Communications*, *2022*(1), 1–14.

Li, L., Tang, G., Shi, Z., Ding, H., Liu, C., Cheng, D., Zhang, Q., Yin, L., Yao, Z., & Duan, L. (2021). Transfer-printed, tandem microscale light-emitting diodes for full-color displays. *Proceedings of the National Academy of Sciences*, *2021*(18).

Li, R., Wang, L., & Yin, L. (2018). Materials and devices for biodegradable and soft biomedical electronics. *Materials*, *2018*(11).

Li, H., Xu, Y., Li, X., Chen, Y., Jiang, Y., Zhang, C., Lu, B., Wang, J., Ma, Y., Chen, Y., Huang, Y., Ding, M., Su, H., Song, G., Luo, Y., & Feng, X. (2017). Epidermal inorganic optoelectronics for blood oxygen measurement. *Advanced Healthcare Materials*, *6*(9), 1601013. Available from https://doi.org/10.1002/adhm.201601013.

Lu, B., Chen, Y., Ou, D., Chen, H., Diao, L., Zhang, W., Zheng, J., Ma, W., Sun, L., & Feng, X. (2015). Ultra-flexible piezoelectric devices integrated with heart to harvest the biomechanical energy. *Scientific Reports*, *2015*(1), 1–9.

Lu, L., Gutruf, P., Xia, L., Bhatti, D. L., Wang, X., Vazquez-Guardado, A., Ning, X., Shen, X., Sang, T., Ma, R., Pakeltis, G., Sobczak, G., Zhang, H., Seo, Do, Xue, M., Yin, L., Chanda, D., Sheng, X., Bruchas, M. R., & Rogers, J. A. (2018). Wireless optoelectronic photometers for monitoring neuronal dynamics in the deep brain. *Proceedings of the National Academy of Sciences of the United States of America*, *115*(7), E1374–E1383. Available from https://doi.org/10.1073/pnas.1718721115, http://www.pnas.org/content/pnas/115/7/E1374.full.pdf.

Lu, L., Yang, Z., Meacham, K., Cvetkovic, C., Corbin, E. A., Vázquez-Guardado, A., Xue, M., Yin, L., Boroumand, J., Pakeltis, G., Sang, T., Yu, K. J., Chanda, D., Bashir, R., Gereau, R. W., Sheng, X., & Rogers, J. A. (2018). Biodegradable monocrystalline silicon photovoltaic microcells as power supplies for transient biomedical implants. *Advanced Energy Materials*, *8*(16), 1703035, Article 201703035. Available from https://doi.org/10.1002/aenm.201703035.

Mannoor, M. S., Tao, H., Clayton, J. D., Sengupta, A., Kaplan, D. L., Naik, R. R., Verma, N., Omenetto, F. G., & McAlpine, M. C. (2012). Graphene-based wireless bacteria detection on tooth enamel. *Nature Communications*, *2012*(1), 1–9.

Moreno, S., Keshtkar, J., Rodriguez-Davila, R. A., Bazaid, A., Ibrahim, H., Rodriguez, B. J., Quevedo-Lopez, M. A., & Minary-Jolandan, M. (2020). Bioelectronics on mammalian collagen. *Advanced Electronic Materials*, *6*(8), Article 202000391. Available from https://doi.org/10.1002/aelm.202000391.

Mostafalu, P., Nezhad, A. S., Nikkhah, M., & Akbari, M. (2016). *Flexible electronic devices for biomedical applications* (pp. 341–366). Springer Science and Business Media LLC. Available from 10.1007/978-3-319-32180-6_16.

Park, M., Park, Y. J., Chen, X., Park, Y. K., Kim, M. S., & Ahn, J. H. (2016). MoS2-based tactile sensor for electronic skin applications. *Advanced Materials*, *28*(13), 2556–2562. Available from https://doi.org/10.1002/adma.201505124, http://www3.interscience.wiley.com/journal/119030556/issue.

Pham, T. A., Nguyen, T. K., Vadivelu, R. K., Dinh, T., Qamar, A., Yadav, S., Yamauchi, Y., Rogers, J. A., Nguyen, N. T., & Phan, H. P. (2020). A versatile sacrificial layer for transfer printing of wide bandgap materials for implantable and stretchable bioelectronics. *Advanced Functional Materials*, *30*(43), Article 202004655. Available from https://doi.org/10.1002/adfm.202004655.

Rajaram, K., Yang, S. M., & Hwang, S.-W. (2022). Transient, biodegradable energy systems as a promising power solution for ecofriendly and implantable electronics. *Advanced Energy and Sustainability Research*, *2022*, 2100.

Renault, J. P., Bernard, A., Juncker, D., Michel, B., Bosshard, H. R., & Delamarche, E. (2002). Fabricating microarrays of functional proteins using affinity contact printing. *Angewandte Chemie - International Edition*, *41*(13), 2320–2323. Available from https://doi.org/10.1002/1521-3773(20020703)41:13<2320::AID-ANIE2320>3.0.CO;2-Z.

Riemer, R., & Shapiro, A. (2011). Biomechanical energy harvesting from human motion: theory, state of the art, design guidelines, and future directions. *Journal of Neuroengineering and Rehabilitation*, *8*(1), 22. Available from https://doi.org/10.1186/1743-0003-8-22.

Rogers, J. A., Ghaffari, R., & Kim, D. H. (2016). *Stretchable bioelectronics for medical devices and systems microsystems and nanosystems*. Springer International Publishing. Available from 10.1007/978-3-319-28694-5.

Schiele, N. R., Corr, D. T., Huang, Y., Raof, N. A., Xie, Y., & Chrisey, D. B. (2010). Laser-based direct-write techniques for cell printing. *Biofabrication*, *2010*(3).

Shin, G., Gomez, A. M., Al-Hasani, R., Jeong, Y. R., Kim, J., Xie, Z., Banks, A., Lee, S. M., Han, S. Y., & Yoo, C. J. (2017). Flexible near-field wireless optoelectronics as subdermal implants for broad applications in optogenetics. *Neuron*, *2017*(3), 509–521.

Shin, J., Liu, Z., Bai, W., Liu, Y., Yan, Y., Xue, Y., Kandela, I., Pezhouh, M., MacEwan, M. R., & Huang, Y. (2019). Bioresorbable optical sensor systems for monitoring of intracranial pressure and temperature. *Science Advances*, *2019*(7).

Sim, K., Rao, Z., Li, Y., Yang, D., & Yu, C. (2018). Curvy surface conformal ultra-thin transfer printed Si optoelectronic penetrating microprobe arrays. *NPJ Flexible Electronics*, *2018*(1), 1–6.

Singh, R., Bathaei, M. J., Istif, E., & Beker, L. (2000). A review of bioresorbable implantable medical devices: materials, fabrication, and implementation. *Advanced Healthcare Materials*, *2020*(18).

Solis, D. J., Coyer, S. R., García, A. J., & Delamarche, E. (2010). Large-scale arrays of aligned single viruses. *Advanced Materials*, *22*(1), 111–114. Available from https://doi.org/10.1002/adma.200902086Switzerland, http://www3.interscience.wiley.com/cgi-bin/fulltext/122589009/PDFSTART.

Song, E., Chiang, C. H., Li, R., Jin, X., Zhao, J., Hill, M., Xia, Y., Li, L., Huang, Y., Won, S. M., Yu, K. J., Sheng, X., Fang, H., Alam, M. A., Huang, Y., Viventi, J., Chang, J. K., & Rogers, J. A. (2019). Flexible electronic/optoelectronic microsystems with scalable designs for chronic biointegration. *Proceedings of the National Academy of Sciences*, *116*(31), 15398–15406. Available from https://doi.org/10.1073/pnas.1907697116.

Song, K., Han, J. H., Lim, T., Kim, N., Shin, S., Kim, J., Choo, H., Jeong, S., Kim, Y. C., Wang, Z. L., & Lee, J. (2016). Subdermal flexible solar cell arrays for powering medical electronic implants. *Advanced Healthcare Materials*, *5*(13), 1572–1580. Available from https://doi.org/10.1002/adhm.201600222, http://onlinelibrary.wiley.com/journal/10.1002/(ISSN)2192-2659.

Stevens, M. M., Mayer, M., Anderson, D. G., Weibel, D. B., Whitesides, G. M., & Langer, R. (2005). Direct patterning of mammalian cells onto porous tissue engineering substrates using agarose stamps. *Biomaterials*, *26*(36), 7636–7641. Available from https://doi.org/10.1016/j.biomaterials.2005.05.001.

Thibault, C., Le Berre, V., Casimirius, S., Trévisiol, E., François, J., & Vieu, C. (2005). Direct microcontact printing of oligonucleotides for biochip applications. *Journal of Nanobiotechnology*, *3*(1). Available from https://doi.org/10.1186/1477-3155-3-7.

Viventi, J., Kim, D.-H., Moss, J. D., Kim, Y.-S., Blanco, J. A., Annetta, N., Hicks, A., Xiao, J., Huang, Y., & Callans, D. J. (2010). A conformal, bio-interfaced class of silicon electronics for mapping cardiac electrophysiology. *Science Translational Medicine*, *2010*(24), 24.

Viventi, J., Kim, D. H., Vigeland, L., Frechette, E. S., Blanco, J. A., Kim, Y. S., Avrin, A. E., Tiruvadi, V. R., Hwang, S. W., Vanleer, A. C., Wulsin, D. F., Davis, K., Gelber, C. E., Palmer, L., Van Der Spiegel, J., Wu, J., Xiao, J., Huang, Y., Contreras, D., … Litt, B. (2011). Flexible, foldable, actively multiplexed, high-density electrode array for mapping brain activity in vivo. *Nature Neuroscience*, *14*(12), 1599–1605. Available from https://doi.org/10.1038/nn.2973.

Wang, Y., Qiu, Y., Ameri, S. K., Jang, H., Dai, Z., Huang, Y. A., & Lu, N. (2018). Low-cost, μm-thick, tape-free electronic tattoo sensors with minimized motion and sweat artifacts. *NPJ Flexible Electronics*, *2*(1), 6. Available from https://doi.org/10.1038/s41528-017-0019-4.

Wigenius, J. A., Fransson, S., von Post, F., & Inganäs, O. (2008). Protein biochips patterned by microcontact printing or by adsorption-soft lithography in two modes. *Biointerphases.*, *3*(3), 75–82. Available from https://doi.org/10.1116/1.2988771, http://scitation.aip.org/getpdf/servlet/GetPDFServlet?filetype = pdf&id = BJIOBN000003000003000075000001&idtype = cvips&prog = normal&doi = 10.1116/1.2988771.

Xie, Y., Wang, H., Cheng, D., Ding, H., Kong, D., Li, L., Yin, L., Zhao, G., Liu, L., & Zou, G. (2021). Diamond thin films integrated with flexible substrates and their physical, chemical and biological characteristics. *Journal of Physics D: Applied Physics*, *2021*(38).

Xu, L., Gutbrod, S. R., Bonifas, A. P., Su, Y., Sulkin, M. S., Lu, N., Chung, H. J., Jang, K. I., Liu, Z., Ying, M., Lu, C., Webb, R. C., Kim, J. S., Laughner, J. I., Cheng, H., Liu, Y., Ameen, A., Jeong, J. W., Kim, G. T., … Rogers, J. A. (2014). 3D multifunctional integumentary membranes for spatiotemporal cardiac measurements and stimulation across the entire epicardium. *Nature Communications*, *5*. Available from https://doi.org/10.1038/ncomms4329.

Yang, Y., Cao, Z., He, P., Shi, L., Ding, G., Wang, R., & Sun, J. (2019). Ti3C2Tx MXene-graphene composite films for wearable strain sensors featured with high sensitivity and large range of linear response. *Nano Energy*, *66*, 104134. Available from https://doi.org/10.1016/j.nanoen.2019.104134.

Yang, Q., Lee, S., Xue, Y., Yan, Y., Liu, T. L., Kang, S. K., Lee, Y. J., Lee, S. H., Seo, M. H., & Lu, D. (2020). Materials, mechanics designs, and bioresorbable multisensor platforms for pressure monitoring in the intracranial space. *Advanced Functional Materials*, *2020*(17), 1910.

Yan, Z., Pan, T., Xue, M., Chen, C., Cui, Y., Yao, G., Huang, L., Liao, F., Jing, W., & Zhang, H. (2017). Thermal release transfer printing for stretchable conformal bioelectronics. *Advanced Science*, *2017*(11).

Yeo, W. H., Kim, Y. S., Lee, J., Ameen, A., Shi, L., Li, M., Wang, S., Ma, R., Jin, S. H., Kang, Z., Huang, Y., & Rogers, J. A. (2013). Multifunctional epidermal electronics printed directly onto the skin. *Advanced Materials*, *25*(20), 2773–2778. Available from https://doi.org/10.1002/adma.201204426.

Ye, R., James, D. K., & Tour, J. M. (2019). Laser-induced graphene: From discovery to translation. *Advanced Materials*, *31*(1). Available from https://doi.org/10.1002/adma.201803621, http://onlinelibrary.wiley.com/journal/10.1002/(ISSN)1521-4095.

Ye, R., James, D. K., & Tour, J. M. (2018). Laser-induced graphene. *Accounts of Chemical Research*, *51*(7), 1609–1620. Available from https://doi.org/10.1021/acs.accounts.8b00084, http://pubs.acs.org/journal/achre4.

Yoon, J., Lee, S. M., Kang, D., Meitl, M. A., Bower, C. A., & Rogers, J. A. (2015). Heterogeneously integrated optoelectronic devices enabled by micro-transfer printing. *Advanced Optical Materials*, *3*(10), 1313–1335. Available from https://doi.org/10.1002/adom.201500365, http://onlinelibrary.wiley.com/journal/10.1002/(ISSN)2195-1071.

Yu, K. J., Kuzum, D., Hwang, S. W., Kim, B. H., Juul, H., Kim, N. H., Won, S. M., Chiang, K., Trumpis, M., Richardson, A. G., Cheng, H., Fang, H., Thompson, M., Bink, H., Talos, D., Seo, K. J., Lee, H. N., Kang, S. K., Kim, J. H., … Rogers, J. A. (2016). Bioresorbable silicon electronics for transient spatiotemporal mapping of electrical activity from the cerebral cortex. *Nature Materials*, *15*(7), 782–791. Available from https://doi.org/10.1038/nmat4624, http://www.nature.com/nmat/.

Yu, J., Ling, W., Li, Y., Ma, N., Wu, Z., Liang, R., Pan, H., Liu, W., Fu, B., & Wang, K. (2021). A multichannel flexible optoelectronic fiber device for distributed implantable neurological stimulation and monitoring. *Small*, *17*(4), Article 2005925. Available from https://doi.org/10.1002/smll.202005925.

Yu, A. A., Savas, T. A., Taylor, G. S., Guiseppe-Elie, A., Smith, H. I., & Stellacci, F. (2005). Supramolecular nanostamping: Using DNA as movable type. *Nano Letters*, *5*(6), 1061–1064. Available from https://doi.org/10.1021/nl050495w.

Yu, A. A., & Stellacci, F. (2007). Contact printing beyond surface roughness: Liquid supramolecular nanostamping. *Advanced Materials*, *19*(24), 4338–4342. Available from https://doi.org/10.1002/adma.200701068.

Yu, A. A., & Stellacci, F. (2006). Stamping with high information density. *Journal of Materials Chemistry*, *16*(28), 2868–2870. Available from https://doi.org/10.1039/b602552h.

Zaaimi, B., Turnbull, M., Hazra, A., Wang, Y., Gandara, C., McLeod, F., McDermott, E., Escobedo-Cousin, E., Idil, A. S., & Bailey, R. (2022). Closed-loop optogenetic control of the dynamics of neural activity in non-human primates. *Nature Biomedical Engineering*, *2022*, 1–17.

Zhang, H., Gutruf, P., Meacham, K., Montana, M. C., Zhao, X., Chiarelli, A. M., Vázquez-Guardado, A., Norris, A., Lu, L., & Guo, Q. (2019). Wireless, battery-free optoelectronic systems as subdermal implants for local tissue oximetry. *Science Advances*, *2019*(3).

Zhang, Y., Zheng, N., Cao, Y., Wang, F., Wang, P., Ma, Y., Lu, B., Hou, G., Fang, Z., & Liang, Z. (2019). Climbing-inspired twining electrodes using shape memory for peripheral nerve stimulation and recording. *Science Advances*, *2019*(4).

Zhang, K., Jung, Y. H., Mikael, S., Seo, J.-H., Kim, M., Mi, H., Zhou, H., Xia, Z., Zhou, W., & Gong, S. (2017). Origami silicon optoelectronics for hemispherical electronic eye systems. *Nature Communications*, *2017*(1), 1–8.

Zhang, H., Peng, Y., Zhang, N., Yang, J., Wang, Y., & Ding, H. (2022). Emerging optoelectronic devices based on microscale LEDs and their use as. Implantable biomedical applications. *Micromachines*, *2022*(7).

Zhang, M., Wang, X., Huang, Z., & Rao, W. (2020). Liquid metal based flexible and implantable biosensors. *Biosensors*, *2020*(11).

Zhan, X., Si, C., Zhou, J., & Sun, Z. (2020). MXene and MXene-based composites: Synthesis, properties and environment-related applications. *Nanoscale Horizons*, *5*(2), 235–258. Available from https://doi.org/10.1039/c9nh00571d, http://www.rsc.org/journals-books-databases/about-journals/nanoscale-horizons/?id = 8277.

Zhao, R., Guo, R., Xu, X., & Liu, J. (2020). A fast and cost-effective transfer printing of liquid metal inks for three-dimensional wiring in flexible electronics. *ACS Applied Materials & Interfaces*, *12*(32), 36723–36730. Available from https://doi.org/10.1021/acsami.0c08931.